JGR Earth Surface

RESEARCH ARTICLE
10.1029/2025JF008775

Hurricanes Along the Southeast Atlantic Coast Build Marsh Resiliency Through Mineral Sedimentation

Alice Staro[1], Duncan M. FitzGerald[1], Ioannis Y. Georgiou[2], Christopher J. Hein[3], and Zoe J. Hughes[1]

[1]Department of Earth and Environment, Boston University, Boston, MA, USA, [2]The Water Institute, New Orleans, LA, USA, [3]Virginia Institute of Marine Science, William & Mary, Gloucester Point, VA, USA

Key Points:

- Hurricane Irma deposited sediment on S. Atlantic marshes ranging from 0.5 to 8.0 cm in thickness exhibiting heterogeneous cross-shore trends
- Compared to the Gulf Coast, the event layer is coarser with thickness related to exposure to wave energy, flooding duration, and grain size
- This study shows that event sedimentation can be significantly greater than average annual accretion rates, aiding salt marsh resiliency

Supporting Information:

Supporting Information may be found in the online version of this article.

Correspondence to:

A. Staro,
astaro@bu.edu

Citation:

Staro, A., FitzGerald, D. M., Georgiou, I. Y., Hein, C. J., & Hughes, Z. J. (2026). Hurricanes along the Southeast Atlantic Coast build marsh resiliency through mineral sedimentation. *Journal of Geophysical Research: Earth Surface*, *131*, e2025JF008775. https://doi.org/10.1029/2025JF008775

Received 4 AUG 2025
Accepted 13 APR 2026

Author Contributions:

Conceptualization: Duncan M. FitzGerald, Ioannis Y. Georgiou, Christopher J. Hein, Zoe J. Hughes
Data curation: Alice Staro, Ioannis Y. Georgiou, Christopher J. Hein
Formal analysis: Alice Staro, Duncan M. FitzGerald, Zoe J. Hughes
Funding acquisition: Alice Staro, Duncan M. FitzGerald, Ioannis Y. Georgiou, Christopher J. Hein, Zoe J. Hughes
Investigation: Duncan M. FitzGerald, Ioannis Y. Georgiou, Christopher J. Hein
Methodology: Alice Staro, Duncan M. FitzGerald, Ioannis Y. Georgiou, Christopher J. Hein
Project administration: Duncan M. FitzGerald, Ioannis Y. Georgiou, Christopher J. Hein, Zoe J. Hughes
Resources: Alice Staro, Duncan M. FitzGerald, Ioannis Y. Georgiou, Christopher J. Hein

Abstract Salt marshes worldwide are threatened by sea-level rise (SLR) and their survival is linked to the production of belowground biomass and mineral sediment deposition. While hurricanes can pose a significant threat to salt-marsh stability, we show that a single, large magnitude storm can drive deposition surpassing long-term annual accretion. However, the potential thickness of a single hurricane-induced depositional layer remains poorly constrained. Here we assess storm sedimentation (geotechnical characteristics, layer thickness) along the border (∼10 off edge) of salt marshes behind four barrier-island systems (Amelia Island, Sapelo Island, Hilton Head, Cape Romain). Analysis of short cores reveals the presence of Hurricane Irma-related deposits in 32 of 37 sites (0.5–8.0 cm thick) composed of mud to muddy sand. Thickness of the event layer decreases from south (Amelia Island) to North (Cape Romain), corresponding to a decrease in wind velocity, wave energy, and storm surge due to increasing distance from the hurricane path. We found that marsh sites proximal to tidal inlets contained thicker sediment layers with coarser sand than sheltered sites. The heterogeneity in grain size indicates that localized hydrodynamics strongly influence variability in sediment reworking. Regression analyses showed a weak correlation of thickness with wave energy, sand–mud ratio, and storm inundation duration. However, we found a strong relationship ($R^2 = 0.56$) between storm layer thickness and vertical accretion rates at the same sites determined from 210Pb dating Hein et al. (2024), https://doi.org/10.1038/s43247-024-01219-8. This suggests that hurricanes are important contributors to marsh sedimentation, boosting accretion rates and enhancing their resilience to SLR.

Plain Language Summary Climate change and sea-level rise (SLR) threaten the survival of salt marshes, whose resilience is closely tied to the ability to maintain elevation through above ground mineral deposition and belowground biomass. Storms threaten marshes by driving edge erosion and platform scouring through strong winds and high wave energy, while prolonged inundation can lead to vegetation dieback. In contrast, our study reveals that an intense storm event such as Hurricane Irma (September 2017) can deliver large quantities of sediment to the marsh edge. Furthermore, it demonstrates that deposition during a single event can reach 8 cm thick, boosting vertical accretion rates and enhancing resilience to SLR. We measured the sediment properties and composition of Irma deposits across 37 sites in four backbarrier marshes between Florida and South Carolina. Our analyses show that complex interactions among proximity to the inlet, exposure, storm wave energy and inundation affect sediment dispersal.

1. Introduction

Salt marshes are valuable coastal ecosystems that provide nursery grounds and habitat for fish and shellfish (Barbier et al., 2011; Möller et al., 2014), sequester up to 0.1% of the global carbon (Chmura et al., 2003; Ouyang & Lee, 2020), export detritus and nutrients to the coastal ocean (Sousa et al., 2010), and mitigate the effects of flooding and storm surges on the mainland (Möller et al., 2014; Temmerman et al., 2013). Salt marshes are threatened by accelerating sea-level rise (SLR), which is projected to lead to the loss of up to 90% of marshlands worldwide by 2100 (Schuerch et al., 2018).

Deterioration of salt marsh can occur through elevation loss (Cahoon, 2006), lateral edge erosion (Marani et al., 2011), or conversion from high to low marsh (FitzGerald et al., 2008), tidal flats, and/or open water (Ganju et al., 2017; Kirwan & Megonigal, 2013). Although erosion can take place in the absence of SLR (Fagherazzi et al., 2013), this response is thought to be the primary driver of salt marsh loss (e.g., FitzGerald et al., 2021). Moreover, the loss of marshlands increases open-water area and backbarrier tidal prism, thereby threatening the stability of barrier island coasts (FitzGerald et al., 2008, 2021; Wiberg et al., 2020). The loss of marshes as they

Software: Alice Staro, Ioannis Y. Georgiou
Supervision: Duncan M. FitzGerald, Zoe J. Hughes
Validation: Alice Staro
Visualization: Alice Staro, Duncan M. FitzGerald
Writing – original draft: Alice Staro
Writing – review & editing: Duncan M. FitzGerald, Ioannis Y. Georgiou, Christopher J. Hein, Zoe J. Hughes

transform into tidal flats and open water could cost trillions of dollars in property damages and coastal ecosystem services (Jevrejeva et al., 2018; Kulp & Strauss, 2019).

To survive accelerating SLR, marshes must either migrate landward (Schwimmer & Pizzuto, 2000) or accrete vertically through organic accumulation (i.e., biomass production) and inorganic deposition (J. T. Morris et al., 2016). Yet for many coasts globally, landward migration may be prevented by anthropogenic structures (Enwright et al., 2016). Likewise, vertical accretion is often restricted due to limited organic production and/or low or reduced sediment supply (e.g., Hein & Kirwan, 2024; Torio & Chmura, 2013; Weston, 2014). However, the survival of some marshes is enhanced by the episodic delivery of sediment during high-energy events (e.g., Stumpf, 1983), such as tropical and extratropical storms, hurricanes, and river flooding. Indeed, sediment deposition associated with a single event can be responsible for accumulation equating to decades of annual accretion, thereby enhancing marsh resilience to climate change and accelerating SLR (Baustian & Mendelssohn, 2015, 2018; Cahoon et al., 1995; FitzGerald et al., 2020; Kirwan & Guntenspergen, 2010; McKee & Cherry, 2009; R. E. Turner et al., 2006; Tweel & Turner, 2012). Several studies have described the spatial distribution and thickness of sediment layers deposited on marshes during the passage of frontal systems (Reed, 1989), tropical storms (Goodbred & Hine, 1995), and numerous hurricanes (e.g., R. E. Turner et al., 2006; Tweel & Turner, 2012). Detailed measurements along the Louisiana coastal plain revealed that approximately 131×20^6 metric tons of sediment were deposited by Hurricanes Katrina and Rita in 2005 (R. E. Turner et al., 2006). Later, McKee and Cherry (2009) showed that Hurricane Katrina also added 3–8 cm of sediment along the border of northeast Lake Pontchartrain (Louisiana) shore and at the mouth of the Pearl River in Mississippi. By way of comparison, the maximum hurricane-related deposition due to storm surge waters *measured to date* on East Coast marshes was an order of magnitude lower (0.3–0.8 cm at Cedar Island, North Carolina (NC); Cahoon, 2003). Importantly, it has been shown that the addition of new sediment to the marsh platform provides a nutrient-rich layer of soil that can boost overall post-storm primary production (Baustian & Mendelssohn, 2015) by allowing root expansion (McKee & Cherry, 2009) and improving soil properties (i.e., increasing Redox potential, reduce sulfide in porewaters, delivering bio-limiting nutrients such as phosphorus; Baustian & Mendelssohn, 2018). The increase in belowground root and rhizome density can boost elevation and reduce the erodibility of the marsh (Cherry et al., 2009; Feagin et al., 2009; Howes et al., 2010; J. T. Morris et al., 2002; Nyman et al., 1993; R. Turner et al., 2002).

While hurricane sedimentation studies (using surface elevation table-marker horizon method) along the New Jersey and New York coasts after Hurricane Sandy showed wide variability of elevation gain and loss with no net trend (e.g., Yeates et al., 2020), other studies have also proven that storm-driven sedimentation can boost accretion rates (e.g., J. T. Morris et al., 2020; Nyman et al., 1995; Roman et al., 1997). Recent work along the U.S. Southeast (Georgia Bight) indicates that vertical accretion can be strongly enhanced at marsh edges abutting open water and tidal inlets (Hein et al., 2024). Using ^{210}Pb and ^{137}Cs profiles from 16 sediment cores collected near platform margins behind four barrier-island systems, Hein et al. (2024) reported that most edge sites accrete faster than contemporary relative SLR, with the highest rates occurring adjacent to large bays and inlets. They interpreted this spatial pattern as evidence that episodic substantive inputs of allochthonous mineral sediment can locally increase marsh resilience at exposed edges, while more protected interior marshes receiving less sediment may remain closer to a drowning threshold. Importantly for interpreting these elevated accretion rates, Hein et al. also noted near-surface mineral-dominated event layers at several rapidly accreting sites, consistent with storm-driven sediment delivery. Apart from beneficial sedimentation, storms may also cause negative impacts to backbarrier marshes (Howes et al., 2010; Morton & Barras, 2011). For example, heightened waves during storms can increase the rate of marsh edge erosion (Bendoni et al., 2014, 2019; Bloemendaal et al., 2021; Feagin et al., 2009; Leonardi & Fagherazzi, 2015; Marani et al., 2011) as well as scour and remove portions of the marsh surface (Howes et al., 2010). The aftermath of storms has also been linked to shrinkage, compaction, and subsidence of soil (e.g., Cahoon, 2006), and overall degradation of the marsh (FitzGerald & Hughes, 2019; Howes et al., 2010; Morton & Barras, 2011). However, investigators have also shown that material eroded from marsh edges during storms may be delivered back onto the marsh platform (Cahoon, 2006; Hopkinson et al., 2018), thereby aiding vertical accretion and reducing the vulnerability to SLR (Kirwan et al., 2016) and boosting primary production and organic deposition (Baustian & Mendelssohn, 2015).

Although research on hurricane impacts on Atlantic coast marshes increased after Hurricane Sandy (2012) (e.g., Brandon et al., 2014; Elsey-Quirk, 2016), most work over the past decades has focused on the U.S. Gulf Coast, primarily in Louisiana, while salt marshes along the U.S. The East Coast has received comparatively less attention (e.g., Cahoon, 2003; Gardner et al., 1991). Moreover, although the post-storm monitoring in Louisiana has yielded important models for hurricane sedimentation, the transferability of this knowledge is not well-established nor confirmed. Gulf Coast wetlands occur in microtidal, low-energy settings fronted by broad, shallow-water bays and often experience diurnal tides. During storms, large waves easily suspend bay muds and surge waters carry the sediment onshore, depositing it on landward marshes (Georgiou, FitzGerald, Sakib, et al., 2024; Liu et al., 2018). Conversely, expansive Atlantic Coast marshes occur in mostly mixed-energy settings (sensu: M. Hayes, 1979) protected by continuous barrier island chains, which serve to reduce the effects of storm wave energy by limiting fetch. Much of the backbarrier in these systems is dominated by sand and coarse silt. Because of these differing geomorphologic and sedimentologic settings, hurricane marsh processes characteristic of the Gulf Coast are not directly comparable.

As a consequence of climate change, increased sea surface temperatures and a warmer Gulf Stream (Woollings et al., 2010) are expected to cause a 40% increase in tropical storms tracking toward Atlantic North America (Balaguru et al., 2023; Mann & Emanuel, 2006). These storms are also expected to be stronger in intensity and frequency (e.g., Bengtsson et al., 2007; Emanuel, 2013; Kossin et al., 2020; Ting et al., 2019) and to travel with reduced forward speed (Gori et al., 2022; Kossin, 2018). Slower-moving storms will produce higher storm surges that will travel further inland and inundate marsh platforms for longer periods. Thus, knowledge of hurricane effects on Atlantic Seaboard marshes is needed to prepare coastal managers and communities for their predicted impact (e.g., Bengtsson et al., 2007; Emanuel, 2013; Kossin et al., 2020; Ting et al., 2019).

Here, we take advantage of the widespread impact of Hurricane Irma to study the effects of a major storm on marsh sedimentation along the southeastern US. In this paper, we identify spatial trends in the thickness and distribution of marsh storm deposits associated with Hurricane Irma covering a 400-km length of coast from northern Florida to central South Carolina (Figure 1). Our study combines numerical simulations of the hurricane's winds, wave energy, and tidal elevations with extensive field studies, including collection of sediment cores 10 ± 1 m from the marsh edge, and laboratory work dedicated to determining the geotechnical properties of the hurricane-deposited layer. Lastly, it explains the exceptionally high accretion rates determined by Hein et al. (2024) at the same marshes through boosted deposition associated with Hurricane Irma. This research provides a large, regional, but high-resolution analysis of the magnitude and spatial variability of Hurricane Irma sedimentation and offers a mechanism by which single events can contribute disproportionately to the multi-decadal accretion signal observed in edge settings.

2. Physical Setting

2.1. The Georgia Bight Coastal Plain

The Georgia Bight, located along the southern US Atlantic coastal plain, extends from Cape Hatteras (NC) to Cape Canaveral (Florida [FL]) and contains a long chain of barrier islands separated by tidal inlets, which front broad salt marshes and estuaries (M. O. Hayes, 1994). The central portion of the Bight is bordered by a shallow continental shelf that influences both wave energy and tidal range (Nummedal, 1978), key factors in determining the shape and length of barrier islands, as well as the size and spacing of tidal inlets (M. O. Hayes, 1994; Nummedal, 1978). Our study area comprises four broad backbarrier marshes behind Cape Romain (SC), Hilton Head Island (SC), Sapelo Island (GA), and Amelia Island (northern FL) (Figure 1). Cape Romain is a cuspate foreland, while the others are beach-ridge barriers, each ~20 km in length with abutting tidal inlets 1–4 km in width. The average deepwater wave height along this sector varies from 1.1 m off Cape Romain to 0.95 m at Amelia Island (Table S2 in Supporting Information S1). Along the same coast, the tidal range increases from 1.6 m at Cape Romain to 2.3 m at Hilton Head and Sapelo Island, reducing to 1.5 m at Amelia Island (Table S2 in Supporting Information S1).

2.2. Storm Conditions

Hurricane Irma made landfall on 10 September 2017 in the lower Florida Keys as a Category 4 storm (Figure 1), with sustained wind speeds of up to 60 m/s. While traveling northward across Florida, Irma lost strength and became a Category 3 hurricane, with sustained winds of up to 51.5 m/s. Early on 11 September, Hurricane Irma moved across the Florida Panhandle, and winds gradually diminished to 26 m/s, with gusts reaching 38.5 m/s. The hurricane moved toward Alabama, weakening while traveling northwest into the continental US until it dissipated on 13 September over southeastern Missouri. Although Hurricane Irma traveled along the western coast of

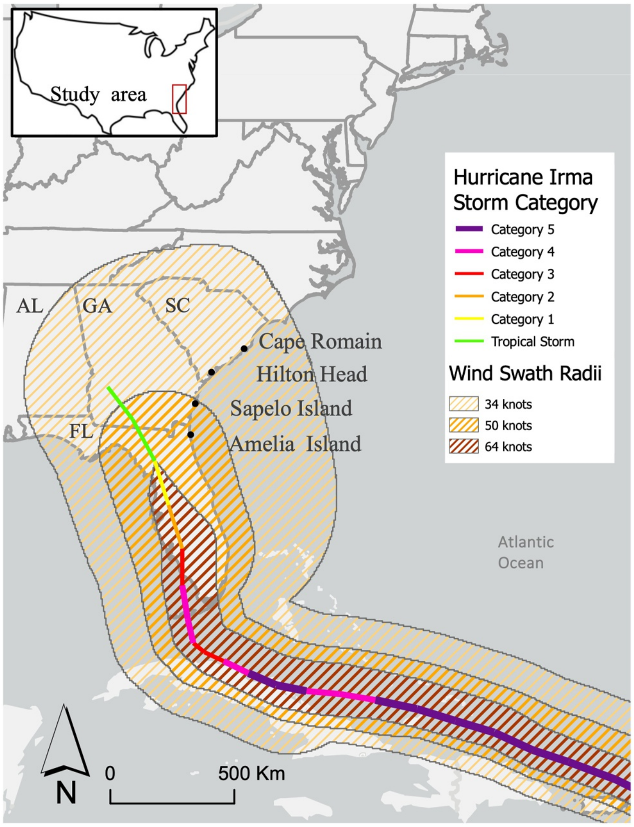

Figure 1. Map of the southeastern United States showing the wind swath and intensity of Hurricane Irma, plotted alongside the locations of our study sites. The intensity of Hurricane Irma decreased from Category 4 to tropical storm while traveling across the Florida Panhandle. Amelia Island and Sapelo Island were in the 50 knots radius, while Hilton Head and Cape Romain are located within the 34-knot radius. Data from the 2017 Atlantic Hurricane Season (National Hurricane Center, 2018).

Florida, a swath of hurricane-force winds extended eastward to 665 km (360 nautical miles) from the center of the storm (Figure 1). The large size of Irma created strong onshore winds along the length of the Georgia Bight, causing high storm surges from Florida to South Carolina (Cangialosi et al., 2018).

The strong winds also produced storm surges lasting several days (Figure S1 in Supporting Information S1). Water levels began to rise a few days before the actual landfall, steadily increasing and peaking on 11 September. These then promptly decreased (comparing observed to predicted water levels, Figure S1 Supporting Information S1) in the hours following the passage of the hurricane. By 12 September, the storm surge had been completely attenuated. On average, the Irma storm surge varied across barrier islands: water levels above MLLW ranged from an average of 3.7 m at Hilton Head, with heights of 3.4 and 3.1 m at Sapelo Island and Amelia Island, to a low of 2.8 m at Cape Romain, the most northerly site (Table S2 in Supporting Information S1).

3. Methods

3.1. Field Data Collection and Core Sampling

Field data were collected in December 2017, three months after the passage of Hurricane Irma, and before the beginning of the growing season. The presence of an undisturbed storm layer and the absence of bioturbation were confirmed prior to data collection via a small trench dug proximal to the target coring sites (Figure 2). Although visibly bioturbated sites were avoided during sampling, two cores contained deep crab burrows, and, thus, the secondary archival cores were used for the analyses.

Despite the 3-month delay, the storm layer had only partially dewatered and compacted in comparison to deeper and denser background marsh sediment (See results section for bulk density as proxy to identify the hurricane layer).

A total of 37 stations were sampled across Cape Romain (10), Hilton Head (9), Sapelo Island (8), and Amelia Island (10) (Figure 3). At each, pairs of short (~50 cm) cores were collected, with one later sampled and the other preserved for archival. Cores were extracted using a Dutch Corer, transferred to a PVC casing, stored horizontally, and kept refrigerated to maintain sediment stability and to prevent algal growth and root decomposition (Mudroch & Bourbonniere, 1994; Tuit & Wait, 2020). Marsh surface elevation at the coring sites was measured using RTK-GPS (Topcon Hiper Lite II global positioning system with integrated real-time kinematics) and corrected using the National Oceanic and Atmospheric Administration Online Positioning User Service (OPUS).

Coring stations (taken 10 ± 1 m of marsh edge) were chosen at approximately equidistant points along two backbarrier transects from the mainland to the barrier islands at each of the four barrier systems, all approximately within 10 m from the edge. These naturally represent a wide range of orientations and fetches, allowing us to examine the role of backbarrier configuration in sediment delivery. We included sites in channels that were generally oriented WNW-ESE (Figure 3), that is, with marsh edges open to the direction of winds and waves generated by Hurricane Irma. Hence, sites may be located on the leeward (e.g., C9) and windward side (e.g., S6) of channels, or on marsh edges fronted by a relatively uniform and flat intertidal zone and proximal to smaller secondary channels (e.g., H4). Other sites are in more protected regions, such as those directly behind the emerged bar of a tidal channel or behind an oyster reef. These much more sheltered sites exhibit a shorter fetch and likely experienced lower wave energy. Finally, other sites (e.g., H1, S5, and A2) are located near major tidal inlets, and are therefore less sheltered, have larger fetch, and experience higher wave energy.

3.2. Sample Extraction and Laboratory Analyses

Cores were cleaned to remove any oxidized surface layer along the split side of the core and to provide a fresh non-oxidized surface for extracting samples for analyses. They were then visually inspected for macroscopic

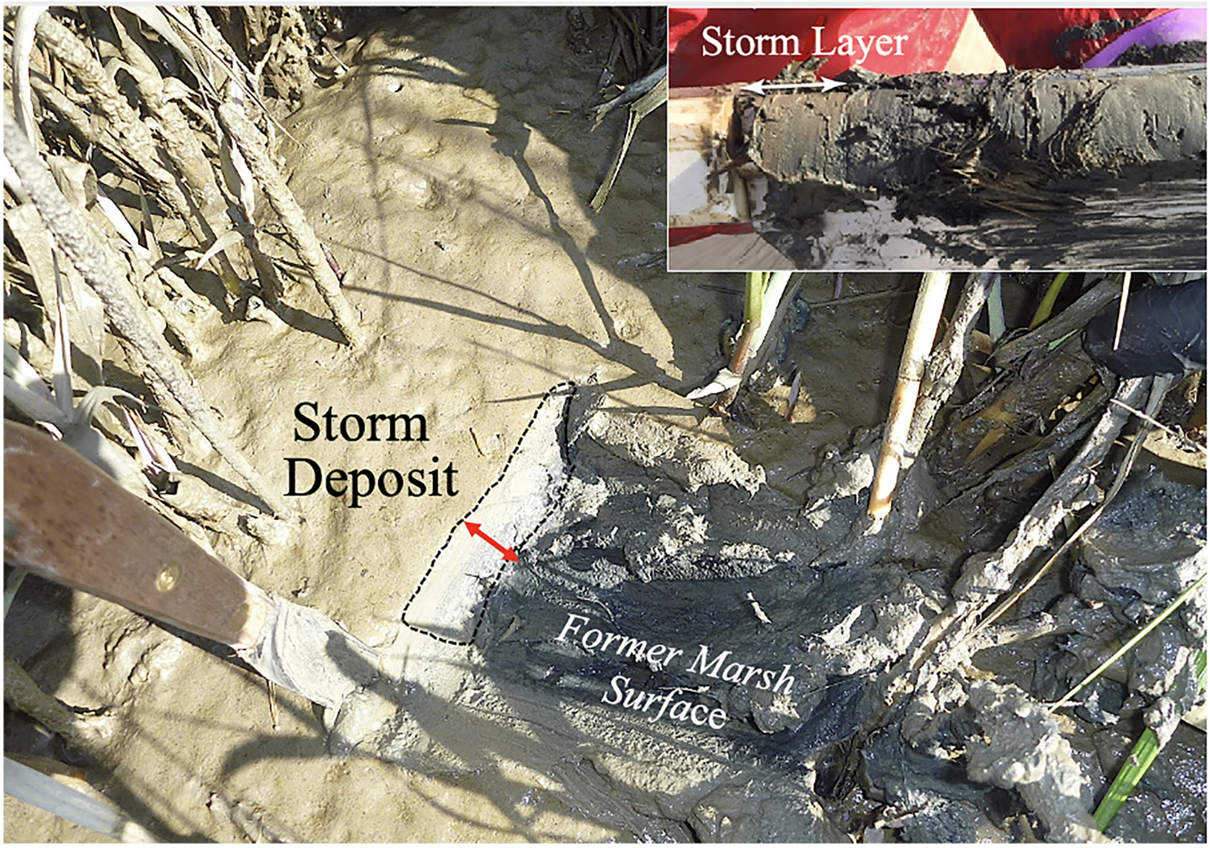

Figure 2. Identification of a non-bioturbated hurricane deposit (~2 cm thick) through exposure of pre-storm marsh surface. The red arrow indicates a break in the sedimentation. The homogeneous nature of the top 4 cm of the core (white arrow) supports the lack of sediment reworking post-Hurricane Irma passage.

features, including laminations, root density, and grain-size trends, and assigned colors using the Munsell Soil Color Chart (Munsell, 2000). The duplicate, archive cores were x-rayed using a high-frequency portable veterinarian X-Ray generator (HF100+, MinXray brand), housed at the Virginia Institute of Marine Science. Radiographs have been widely applied in the study of varves (e.g., Dallimore et al., 2005), paleotempestites in coastal zones (e.g., Collins et al., 1999; Scott et al., 2003), and storm deposits in washover fans (e.g., Chaumillon et al., 2017) as a non-destructive tool able to highlight contrasts in density and composition, accentuating laminations that might not be visible to the naked eye.

Each core was sliced into 1-cm-thick intervals: 10 consecutive slices covered the upper 10 cm, where the hurricane deposit was most likely to occur, and additional 1 cm slices were taken at lower resolution at 11–12, 14–15, 19–20, 24–25, and 39–40 cm to characterize background sedimentation. When roots or plant parts were present, they were severed in place using either scalpels or small scissors. A total of 15 samples were extracted from each core. Aliquots were analyzed for bulk density and organic content. The latter was accomplished via loss on ignition using standard techniques: 8 hr burn time at 550°C (see Heiri et al., 2001; Plater et al., 2015). Grain size was measured from a second aliquot using a Beckman Coulter LS 13320 (Beckman Coulter GmbH, Krefeld, Germany) laser diffraction particle size analyzer, equipped with an aqueous liquid module and a Polarization Intensity Differential Scatter unit. Prior to analysis, organic matter was removed by applying 2–6 ml of hydrogen peroxide (H_2O_2 at 30% concentration), followed by heating at 60°C for 12 hr, and finally treated with Calgon solution to prevent flocculation. Grain-size distributions were calculated using the Fraunhofer optical model (see de Boer et al., 1987). Grain-size classification followed Wentworth (1922), while statistical summaries were calculated based on the Folk and Ward method (Folk, 1954). See Supporting Information S1 Methods for a more comprehensive discussion on bulk density method quantification and uncertainties.

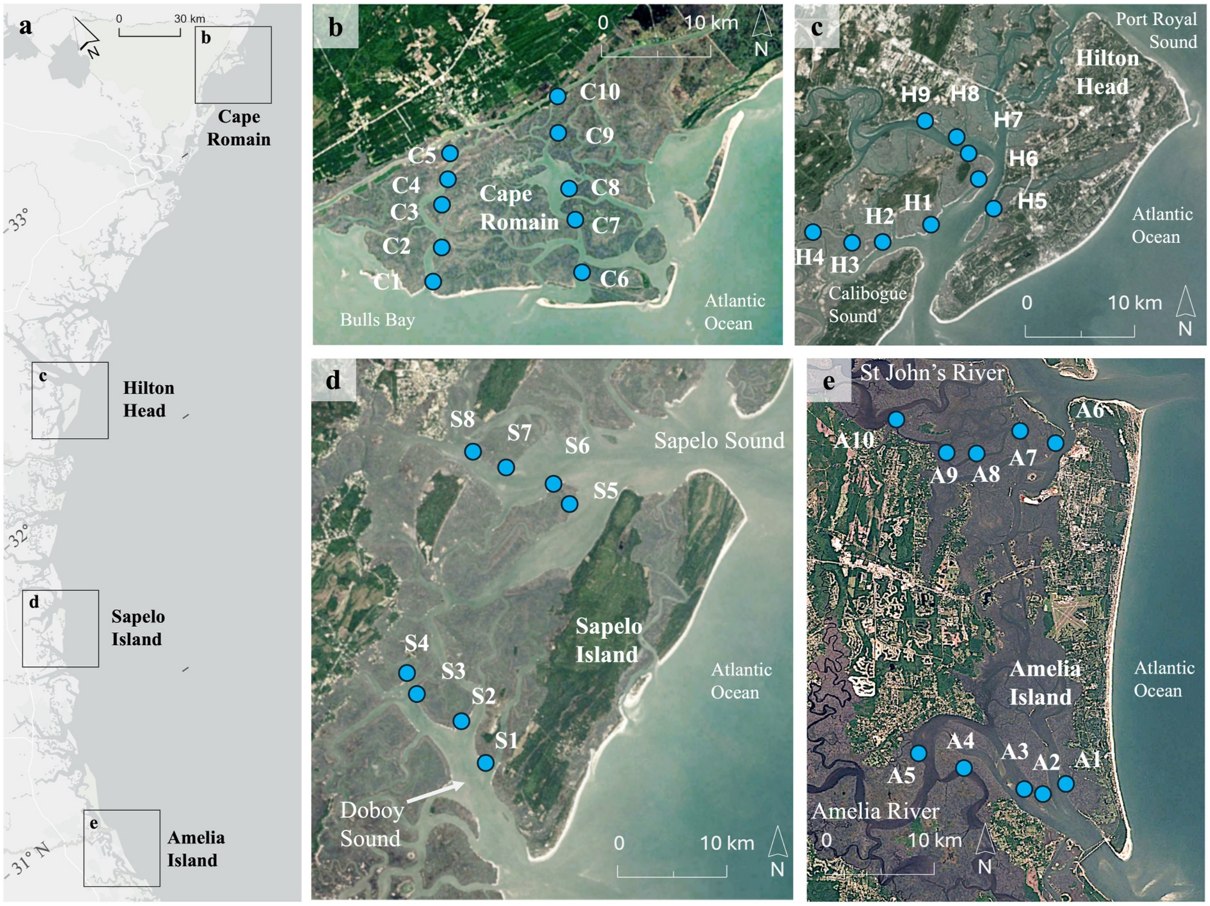

Figure 3. (a) Large scale map showing the location of backbarrier marshes in this study. (b, c, d, e) Sampling site maps indicating core sampling stations (blue circles). The core IDs are assigned based on location and progressively numbered across the two cross-shore transects at each barrier, starting with the first seaward core of the southernmost transect (e.g., C1 = Cape Romain, core no. 1).

3.3. Wave Dynamics

Hurricane Irma conditions were simulated by employing the ADvanced CIRCulation Model (ADCIRC; Luettich et al., 1992; Westerink et al., 1994) coupled with the wave model Simulating WAves Nearshore (SWAN; Booij et al., 1999). The wind re-analysis hindcast fields were prepared for Hurricane Irma in 2017 using Oceanweather Inc. as described in Contreras et al. (2023). Time series were extracted from the model at open-water sites (sounds, bays, channels) adjacent to the coring locations (Figure S2 in Supporting Information S1) including surge height (relative to datum), inundation depth, and wave characteristics (significant wave height, wave period, wave direction) every 20 min.

Because the bathymetry in the model is referenced to the North American Vertical Datum of 1988 (NAVD88), all storm surge heights were reported in NAVD88 to ensure direct comparability with elevation measurements at each of our sites and to accurately represent the inundation magnitude and duration. Wave directions from SWAN are expressed in nautical convention (i.e., the direction where the wind or the waves come from, measured clockwise from geographic North). Wave energy was calculated using linear wave theory using the equation below:

$$E = (1/16) \cdot \rho \cdot g \cdot Hs^2$$

where: ρ is water density, equal to 1,025 kg/m^3, g is gravitational acceleration, equal to 9.81 m/s^2, and Hs is significant wave height in m. The time series model output that was used in our study is available in an online repository (Georgiou & Diaz Garcia, 2025).

3.4. Statistical Analyses

We used single and multivariate iterative linear regressions to explore the relationship between Hurricane Irma deposits and the physical factors affecting sedimentation. Wave energy is used as a proxy for potential suspended sediment, sand abundance is represented by including a proximity to sand shoals and sandy substrates, and duration of inundation is used to provide a measure of potential settling of the suspended sediment. Wave energy was determined at open-water sites adjacent to our coring locations, using hydrodynamic modeling output (from Contreras et al., 2023).

Models were built according to correlation with the target dependent variable (thickness; see correlation matrix Figure S3 in Supporting Information S1), starting with the highest correlation and adding further independent variables based on improvement of the adjusted R^2, the p-value of the model, and associated p-values.

In addition to linear regressions, we performed a Linear Discriminant Analysis (LDA). This statistical tool maximizes the separation among groups while reducing the variation within each group. It is a technique that highlights groups within a data set that share similar features by forming linear combinations based on selected attributes. In this data set, we identify the type of sediment and its distribution across the transects, the range of sediment thicknesses measured in the cores, and the overall storm conditions (here represented by deposit thickness, wave energy, duration of inundation, and sand–mud ratio).

4. Results

4.1. Wave Simulations

Due to the high variability in fetch and exposure, wave energy varies greatly among the study sites, ranging from 50 J/m^2 (Cape Romain C10) to 827 J/m^2 (Sapelo Island, S7) (Figure 4). These data illustrate that, as the storm was crossing the Florida Panhandle, high wave energy was approaching from the southeast and east-southeast, and as the storm traveled northward and inland, wind velocities and wave energies reduced in magnitude and became more aligned with the trend of the coast.

4.2. Hurricane Irma Depositional Layer Thickness

We observed sediments interpreted to be associated with Hurricane Irma deposition at 32 out of 37 sites (Table 1). This unit varied in thickness from 0.5 cm at Cape Romain station C4 to 8.0 cm at Sapelo Island station S6 (Figure 5). All sites at Amelia Island (10) and Sapelo Island (8) contained Irma deposits, and eight out of nine sites had a hurricane layer at Hilton Head. However, at Cape Romain, a deposit was identified at only six out of 10 sites.

We found that the thickness of the hurricane deposit generally increased with proximity to the hurricane's track, with Amelia Island and Sapelo Island having the highest averages (2.7 and 3.5 cm, respectively) versus Hilton Head and Cape Romain (and 2.16 and 1.0 cm, respectively), the lowest (Figure 6a). The storm deposit, exhibiting a maximum thickness of 8 cm at Sapelo Island, was documented by visual observations at the coring sites, high-resolution down-core analyses, and radiographs, which helped to delineate the storm deposit from background marsh sediment (e.g., Castagno et al., 2021; Goni et al., 2007).

4.3. Geotechnical Parameters of the Hurricane Irma Layer

The Hurricane Irma layer consists mostly of finely laminated silt and clay, matching field observations (Figure 2) and previous descriptions by King et al. (2019). The horizontal laminae, resulting from variations in mineral composition and density, can be detected both in radiographs and by the naked eye (Figure S6 in Supporting Information S1). The storm layer tends to exhibit a dark color (Munsell: 2.5 Y 3/2), and lacks the rich organic content (roots, plant parts, shells) that characterizes standard marsh sediment (i.e., the lower portion of the cores). When exposed, the surface of the storm layer is often oxidized to yellow-mustard-beige hues, whereas the background marsh sediment oxidizes to rust-dark orange colors.

Most of the samples identified as belonging to the hurricane layer contain a higher percentage of mud compared to sand (low sand-to-mud ratio, Table 1). However, sandier deposits occur at a subset of sites, consistent with proximity to stronger hurricane forcing (e.g., wave energy, Figure 4) and/or to sandy sediment sources such as tidal inlets and adjacent sand bodies (Figures S7 and S8 in Supporting Information S1).

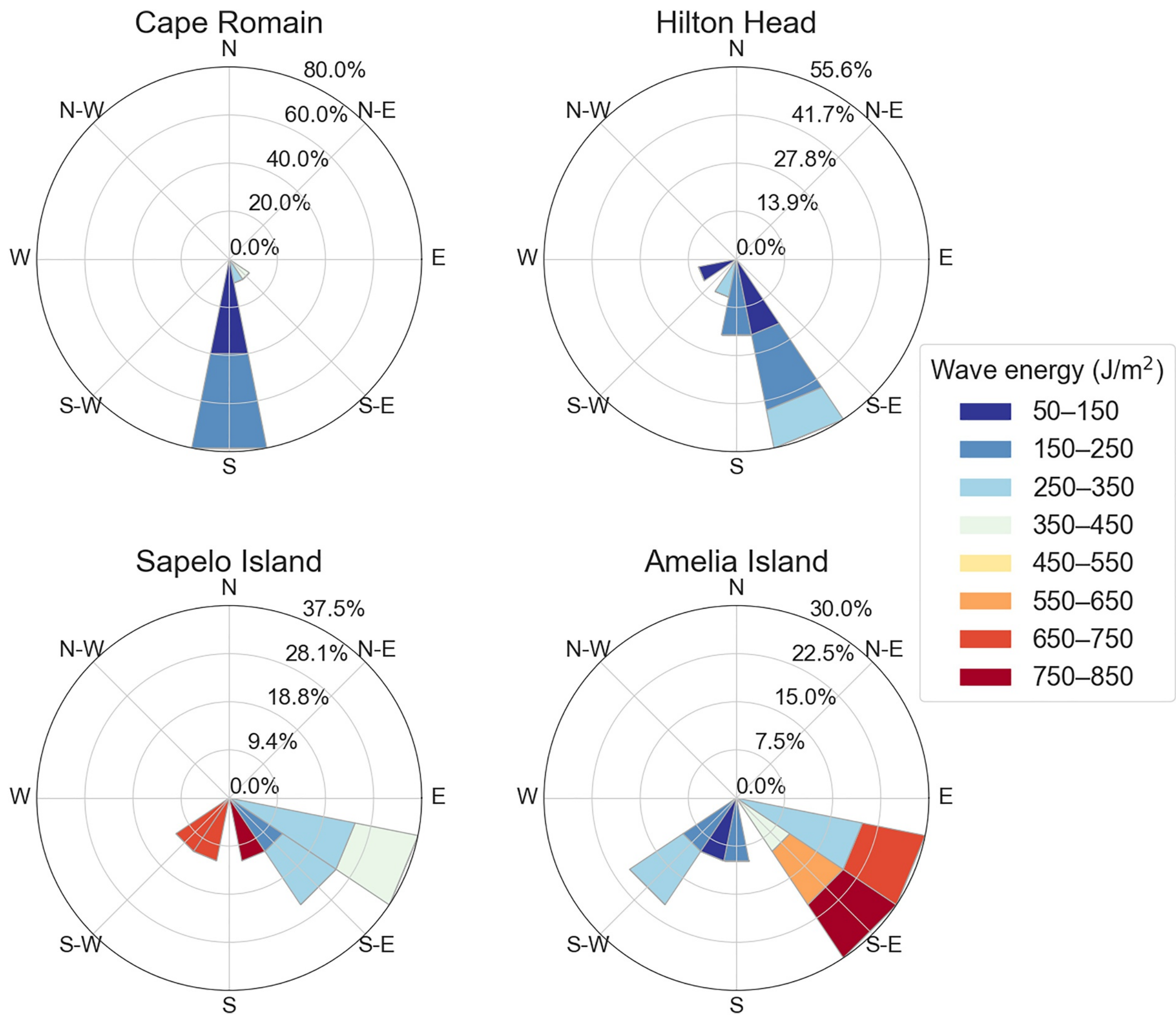

Figure 4. Wave energy rises diagrams for Amelia Island, Sapelo Island, Hilton Head Island, and Cape Romain. Each compass vector shows the maximum wave energy magnitude (colored legend) and direction for wave energy within our numerical simulations for Hurricane Irma. Each concentric circle shows the frequency of occurrences in each wave-energy bin (as a percentage of total measurements). See Figure S4 in Supporting Information S1 for cumulative wave energy for the period 10–12 September 2017.

In general, across sites, the coarser fraction contains sand (up to 60%, from very coarse to very fine sand), although in most samples, silt and clay dominate making up more than 60% of the deposit (Figures S9 and S10 in Supporting Information S1). Overall trends in organic content and bulk density (Figures S11 and S12 in Supporting Information S1) mimic the distribution shown by other authors for marsh sediments (e.g., Bloemendaal et al., 2021; Grigal et al., 1989; Jeffrey, 1970; J. T. Morris et al., 2016).

4.4. Hurricane Layer Stratigraphy

Hurricane Irma deposits in our study area consist of variable proportions of mud (silt and clay) and sand, comprising single or mixed layers (Figure 6c). The stratigraphy of individual deposits reflects the sediment source and hydrodynamic energy. Larger percentages of sand were located at sites proximal to sandy channel bottoms and tidal flats (e.g., H7), where sufficient wave energy and tidal currents suspended sand off the bottom and surge waters transported it onto the marsh (e.g., de Groot et al., 2011). Muddier layers occurred predominantly in low-energy, protected sites where fetch-limited waves acted upon largely muddy bottom sediments. Two such examples occur in the landward ends of the Amelia Island transects at sites A4 and A10 (89% and 93% mud, respectively, Figure S9 in Supporting Information S1, Table 1). Sites with the highest sand content were found

Table 1
Physical and Hydrodynamic Characteristics of Hurricane-Deposited Sediment Layers

Core ID	Elevation [m] NADV88	Distance to major inlet [km]	Thickness [cm]	Sand content (%)	Mud content (%)	Sand–mud ratio	Duration [hrs]	Wave energy [J/m^2]
A1	0.44	5.20	3.5	16.20	83.80	0.19	24.0	686.3
A2	0.38	5.10	2.5	34.70	65.30	0.53	23.0	812.6
A3	0.36	6.20	4	60.42	39.58	1.53	22.3	588.9
A4	0.53	8.60	2	10.90	89.10	0.12	23.7	336.6
A5	0.33	10.80	3.5	55.29	44.71	1.24	23.7	447.5
A6	−0.26	3.32	1	36.38	63.62	0.57	23.7	334.2
A7	0.34	7.30	2.5	6.85	93.15	0.07	22.3	282.1
A8	0.24	9.50	3	9.79	90.21	0.11	10.7	143.5
A9	0.24	11.50	2.5	12.10	87.90	0.14	22.7	244.8
A10	0.43	14.40	2.5	7.00	93.00	0.08	21.7	201.8
C1	0.51	0.60	1	48.89	51.11	0.96	15.0	396.3
C2	0.54	2.40	3	43.18	56.82	0.76	9.0	156.0
C3	0.56	3.90	3.5	31.73	68.27	0.46	10.3	60.1
C4	0.27	6.30	0.5	17.15	82.85	0.21	13.0	134.8
C5	0.57	7.27	1	19.13	80.87	0.24	13.0	197.5
C6	0.37	3.70	1	23.87	76.13	0.31	13.0	281.1
C7	0.43	5.80	0	0	0	0	12.0	171.1
C8	0.17	7.70	0	0	0	0	13.0	193.6
C9	0.54	10.50	0	0	0	0	10.3	65.8
C10	0.44	12.00	0	0	0	0	12.3	50.8
H1	0.60	5.00	3	17.01	82.99	0.21	29.7	331.5
H2	0.54	6.01	2.5	47.34	52.66	0.90	26.0	347.0
H3	0.81	8.30	0	0	0	0	10.0	77.4
H4	0.64	10.70	1	10.78	89.22	0.12	11.7	79.2
H5	0.46	7.60	3	22.89	77.11	0.30	17.7	109.2
H6	0.82	8.40	4	54.19	45.81	1.18	6.7	194.1
H7	0.27	10.10	1	0.49	99.51	0.00	19.7	180.4
H8	0.41	11.30	2	19.39	80.61	0.24	18.3	159.9
H9	0.45	12.60	3	12.40	87.60	0.14	18.7	185.2
S1	0.83	5.05	3	14.86	85.14	0.17	9.0	329.4
S2	0.67	7.40	1	8.04	91.96	0.09	10.3	354.4
S3	0.57	9.54	1	6.82	93.18	0.07	10.7	256.9
S4	0.62	10.64	3	12.91	87.09	0.15	10.7	179.9
S5	0.69	7.95	6	38.43	61.57	0.62	34.7	710.2
S6	0.66	9.20	8	47.04	52.96	0.89	35.3	692.0
S7	0.84	11.50	3	45.08	54.92	0.82	32.7	827.2
S8	0.41	13.70	3	20.31	79.69	0.25	21.7	307.9

Note. Core IDs (denote sampling locations; reported metrics on the hurricane layer include deposit thickness, sand and mud content, and sand–mud ratio. Additionally, duration of inundation and wave energy calculated for each sampling station are also reported.

near the entrance to tidal inlets (Figure S13 in Supporting Information S1) such as Nassau Sound at Amelia Island at sampling stations A2 and A3 (34% and 60%, respectively) and Five Fathom Creek Inlet at the western end of Cape Romain (C1), where sand content reached 49% (Figure S9 in Supporting Information S1, Table 1).

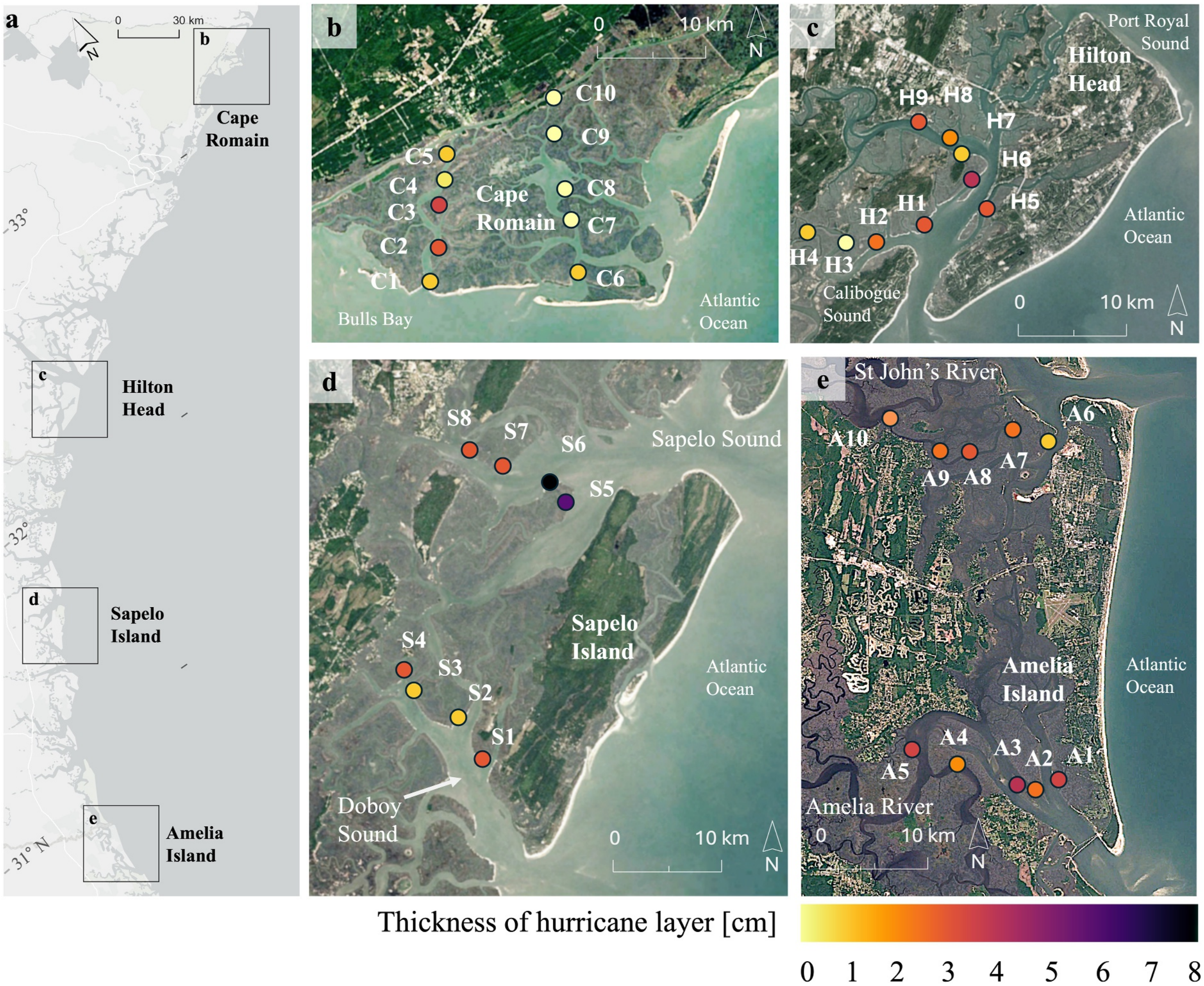

Figure 5. (a) Large scale map and (b–e) Hurricane Irma layer distribution and thickness as determined using multi-proxy characteristics (see Figure S5 in Supporting Information S1). Core locations are shown in circles, in which colors represent the thickness of the hurricane deposit. The core IDs are assigned based on location (e.g., C = Cape Romain) and progressively numbered across the two cross-shore transects at each barrier. The greatest thickness was measured at Sapelo Island stations S6 and S5 (8 and 6.5 cm, respectively). Four cores on Cape Romain (C7, C8, C9, C10) and one core in Hilton Head (H3) did not have a storm deposit.

Hydrodynamic conditions varied during the Irma event, which partially explains the textural changes observed within individual storm layers (e.g., Allen, 2000; de Groot et al., 2011). For example, wave energy and tide levels gradually increased in the days prior to the hurricane passage. However, significant wave heights fell immediately following peak water levels, frequently within a single tidal cycle. Thus, the interplay of relatively slow build-up in wave energy and water levels might explain the initial deposition of muddy sediment at the base of the storm layer, followed by sandier strata, capped at the top by thin, muddier sediments (as recorded in core S5, Figure S14 in Supporting Information S1). These processes, along with hydrodynamics dictated by local wave fetches and exposure, can explain why some storm sequences contain coarsening upward trends while others have fining upward trends, or a combination of both (Figure S15 in Supporting Information S1).

4.5. Absence of Irma Sedimentation

Although Irma deposits were found ubiquitously in all backbarrier systems, four sampling stations at Cape Romain and one at Hilton Head (out of 37) contained no identifiable hurricane layer. This absence might be related to a single cause or combined effects, including the position of the site relative to prevailing winds, the distance from open water (source of sediment), and the presence of sheltering features. For example, robust oyster reefs are known to protect the underlying substrate from erosion and reduce wave energy along adjacent shorelines (Chowdhury et al., 2019; Kitsikoudis et al., 2020; R. L. Morris et al., 2021; Ridge et al., 2015;

10.1029/2025JF008775

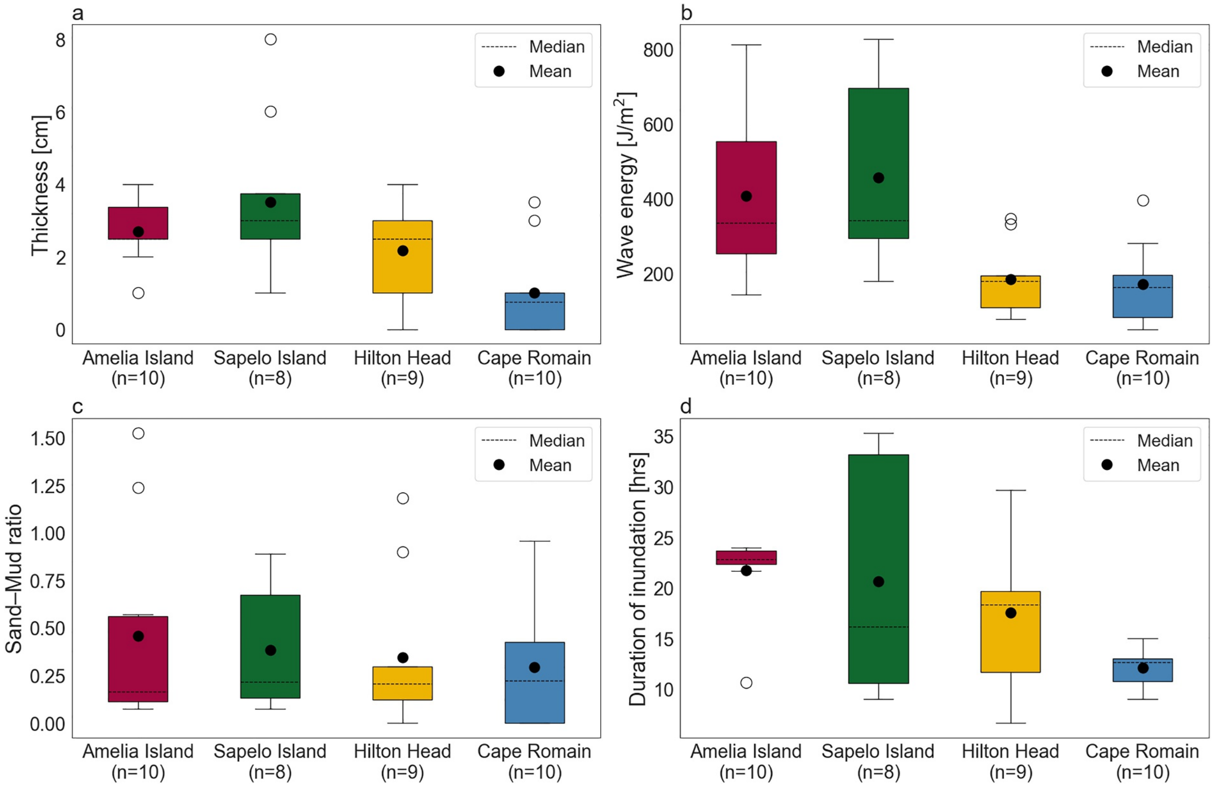

Figure 6. Boxplots (showing range, median, and mean) of the thickness of the layer deposited by Hurricane Irma (a), wave energy (b), sand–mud ratio (c), and duration of inundation (d). Panel (a) shows the combined ranges in thickness of the Hurricane Irma layer atop saltmarshes in four backbarrier areas stretching from northern Florida to central South Carolina. Note the general decrease in thickness from north to south, coincident with greater distance from the hurricane path. Panels (b and c) show generally higher averaged wave energy (b) and higher sand in Amelia Island and Sapelo Island, also a higher sand–mud ratio (c) for the same location. The average duration of inundation (d) has a negative correlation with the distance from the hurricane path. The overall higher averages in the southernmost sites compared to the northern counterparts are consistent with the diminishing energy characterizing the more distal sites.

Styles, 2015; Whitman & Reidenbach, 2012; Wright et al., 1990). Oyster reefs or piles fronting marshes were noted in all four study areas, including those sites where a hurricane layer was identified, but their character and extent were not measured. Their presence, however, would have limited the suspension and conveyance of sediment onto nearby marsh platforms. Likewise, sites further onto the marsh platform and/or on the windward side of channels received more protection during the storm compared to the leeward side and more exposed locations, and thus, less potential sedimentation. For example, Cape Romain was located most distant from the hurricane path and experienced the lowest wave energy compared to the other study areas (Figure 4; Table 1). The four sites containing no observable hurricane deposits (C7, C8, C9, C10) were located along a narrow channel (<200-m wide) with limited fetches and were fronted by a long spit that reduced the attendant ocean wave energy.

4.6. Factors Affecting Deposition and Long-Term Accretion Rates

To further investigate the relative importance of factors affecting the thickness of the hurricane deposits, we chose to look at wave energy, duration of inundation, and sand–mud ratio of the layer by performing an iterative multivariate regression using thickness as the dependent variable. Our regression shows that duration of inundation exhibited the highest individual correlation ($R^2 = 0.33$; p-value = 0.0002; AIC = 132.32) (Figure 7) that slightly improved to 0.48 (p-value = 0.0005; AIC = 127.6) when the effects of wave energy and sand–mud ratio were added (Table S3 in Supporting Information S1). We use the same variables to run a LDA; this too was unable to provide clear separation among the sites (Figure S16 in Supporting Information S1). Lastly, we performed a linear regression analysis between deposit thickness and reported long term accretion rates measured at the same marshes as in this study by Hein et al. (2024) (using ^{210}Pb dating, see Table S4 in Supporting Information S1 in this paper for updated values, and Hein et al., 2024, for details about the methods). We find a strong linear

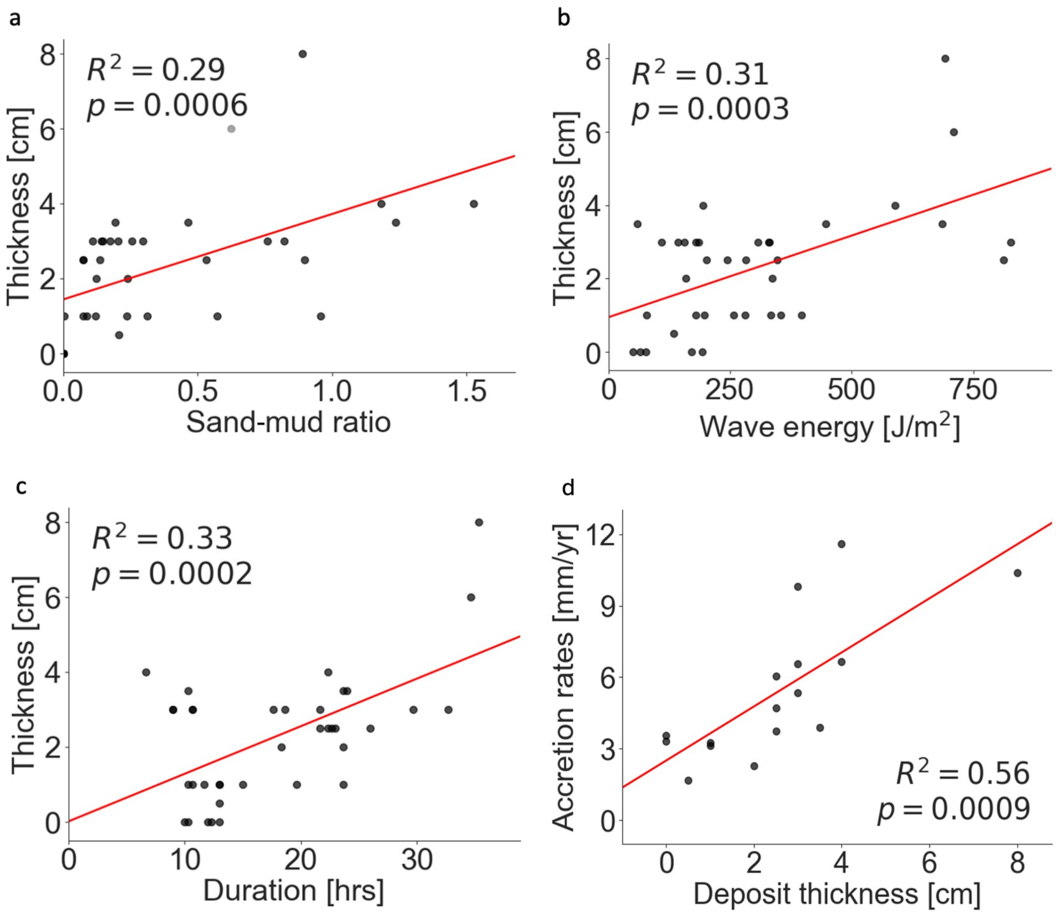

Figure 7. Linear regressions of Hurricane Irma deposit thickness [cm] sand–mud ratio (a), wave energy (b), and Duration of inundation (c). All three predictors show statistically significant correlations, with increasing explanatory power from 29% (a) to 33% (c). (d) Linear regression of multi-decadal marsh accretion rates based on ^{210}Pb dating (Table S1 in Supporting Information S1 after Hein et al., 2024) and the thickness of deposits associated with the passage of Hurricane Irma (this study) (see Tables S3 and S4 in Supporting Information S1 for details). At two sites that Hein identified (at 3.31 and 3.54 mm/yr), we found an absence of hurricane deposit.

relationship between deposit thickness and long-term accretion (R^2 = 0.56; p-value = 0.0001; AIC = 70.25) (Figure 7d, Table S5 in Supporting Information S1).

5. Discussions

Here we explore several aspects of the observed sedimentation event in terms of the general hydrodynamics during Hurricane Irma, trends in the type and quantity of sediment that was deposited, and relationships between physical conditions during the storm and thickness of the associated deposit. As our study is unique, in the sense that it captures the effects of a major storm along a large section of the Atlantic Southeast coast, we further compare our findings to the US Gulf Coast, where other sedimentation studies of large-scale hurricane events have been conducted. Finally, we discuss the impact of hurricanes with respect to salt marsh resilience under a regime of climate change. We note that our results are based on cores collected at a distance of 10 ± 1 m from the marsh edge and therefore interior portions of the marsh would likely have different sedimentation patterns (Moskalski & Sommerfield, 2012).

5.1. Irma Hydrodynamics and Sedimentation Patterns

During fair weather conditions, channel networks represent a preferential pathway for tidal waters to inundate the marsh, allowing very fine sediment to reach the platform (J. T. Morris et al., 2002). Conversely, during high-energy events such as Hurricane Irma, the storm signal overprints the tidal signature, flooding the marsh platform for periods longer than the typical tidal hydroperiod. At the same time, open-ocean waves, acting in conjunction with locally generated wind waves in the backbarrier increase bed shear stresses, producing suspended sediment in greater quantities (Georgiou, FitzGerald, Sakib, et al., 2024) and with a coarser texture. When a storm surge peak coincides with high tide, sedimentation is linked to long periods of standing water and slow drainage, which allows even fine particles (mud) to settle on the marsh surface. In assessing the extent of Hurricane Irma sedimentation along the southeastern Atlantic seaboard, we found a general northerly decrease in both the number of sampling stations containing Irma deposits and deposit thickness (Figures 5 and 6a). Consistent with this interpretation, Irma's forcings declined from south to north (Figures 4 and 6b), corresponding to a decrease in the average duration of storm-driven marsh inundation (Figure 6d).

In contrast, we observed no distinct south-to-north trend in the sand–mud ratio of the hurricane layer, suggesting that deposit texture reflects complex site-specific factors (e.g., local bottom type and proximity to open water) rather than the regional energy gradient alone. For example, a plot of sand content versus distance from inlet (Figure S1 Supporting Information S1) shows higher sand percentages at windward sites, or at sites oriented toward the predominant wind and wave direction, whereas sites on the leeward side of channels record greater mud contents. Interestingly, some sites on the leeward side registered coarser grain size even when located at greater distance from the inlet openings and where wave energies were lower. This would suggest a strong control of sediment delivery pathways or local availability of mobile sediment rather than traditional distance from the inlet. These factors may also help to explain differences between our study results and prior work. At Sapelo Island, R. S. Smith et al. (2024) concluded that no significant sedimentation was linked to Hurricane Irma; however, they based their findings on surface elevation table measurements rather than deposition, and many of their stations were located away from marsh edges where storm sedimentation naturally tends to decrease (Moskalski & Sommerfield, 2012). In contrast, our documentation of the Irma layer is based on timely post-storm field surveys combined with high-resolution station-specific down-core proxies (see Methods and SI Methods). We identified a discrete hurricane layer at 32 out of 37 sites (all located at comparable distances close to the marsh edge) and were able to differentiate the storm layer from background marsh sediment, including at the Sapelo Island GCE-LTER. Field exposures of the muddy deposit at most coring sites indicate widespread blanketing across the study area, even as deposit occurrence and thickness decrease northward. Accordingly, the lack of Irma deposits at several of R. S. Smith et al. (2024) Sapelo Island sites may reflect the SET methodology, their greater protection in areas farther from inlets, or lower concentrations of suspended sediment available for deposition (as observed during Hurricane Sandy; Hu et al., 2018).

Our individual sampling transects spanned an extensive area ranging from 4 to 7 km from the landward side of the barriers to the mainland. Within each of our backbarrier systems, we found no distinct cross-shore pattern in the sediment type or thickness of the hurricane layer. Moreover, our cross-shore data exhibit a great deal of variability as demonstrated by the Amelia Island transects, where thickness values (onshore) from east to west along the southern transect are 3.5, 2.5, 4.0, 2.0, and 3.5 cm, and the adjacent northern transect are 1.0, 2.5, 3.0, 2.5, and 2.5 cm, respectively (Figure S17 in Supporting Information S1). It is well accepted that the thickness and composition of sedimentary deposits are dependent on the source (van Rijn, 1984a, 1984b), energy of the flow, and transport distance (see Reynolds, 2024 for discussion). The lack of cross-shore grain size trends along our transects is thought to be related to proximal changes in bottom sediment type as well as the size, geometry, and orientation of open water, which collectively affect the wave energy and suspension of sediment at each site. The absence of an overall trend also suggests that the sediment source must be local, albeit not necessarily closest to each site, and/or that it is not coming from the same site or environment (such as the nearshore or sound). Nonetheless, the presence of shoals is speculative due to the lack of sampling and direct observation. Therefore, the higher measured sand content may be attributed to exposure to larger open-water areas and greater energy to suspend coarser sediment and/or a proximal sand source. Generally, thicker Irma layers were found on marshes proximal to erodible sediment sources (see Schuerch et al., 2013 for discussion), such as channel bottoms (3 cm, S8), bays (3 cm, S1), and shoals and tidal flats (2.5 cm, H2). Apart from nearby open-water areas, sediment comprising the hurricane layers could also have been derived through cannibalization of the marsh surface or the marsh edge. The coastal ocean, adjacent estuaries, and/or nearby upland regions may have contributed some sediment to the storm deposits; however, the lack of cross-shore trends indicates that no system-wide process clearly overprints local variability. Finally, these findings suggest that the hurricane deposition results from complex interactions of tidal currents, waves, and pathways of sediment delivery, coupled with possible effects of edge erosion, resuspension of marsh platform sediment, and localized morphological variabilities.

Results of iterative regressions show that neither the sand–mud ratio, wave energy, nor duration of inundation has a strong relationship with hurricane layer thicknesses. Instead, the measured thickness values seem to reflect a combination of factors, likely with non-linear dependencies—for example, plant stem densities or canopy height—and physical aspects of the substrate (i.e., grain size variability) and of the storm, including when the highest shear stresses were imparted to the substrate with respect to tidal elevation and effects of tidal currents. These findings, in combination with the lack of observed trends in cross-shore thickness or sand–mud ratio of the deposits, underscore the spatial heterogeneity and localized controls governing storm sedimentation in back-barrier systems.

5.2. Comparison With Other Marshes Along the Atlantic and Gulf Coasts

Our study provides the first measurement of hurricane deposits covering a broad section of the US southern Atlantic coast. Focusing on Hurricane Irma, it includes stations both proximal to storm landfall (Florida) and more distal, which historically have been impacted by fewer hurricanes (Georgia and South Carolina; e.g., Muller & Stone, 2001). Prior to this research, our knowledge of East Coast hurricane sedimentation came primarily from studies of Cedar Island (NC) marsh by Cahoon (2003) and studies focusing on Hurricane Sandy (e.g., Brandon et al., 2014; Cahoon et al., 2019; Elsey-Quirk, 2016). During the mid to late 1990s, Cahoon (2003) monitored the impacts of Hurricanes Emily (1993), Gordon (1994), and Dennis (1999) and found that these minor to moderate storms flooded the Cedar Island marshes, producing 0.3–0.8 cm of sedimentation. In addition, several numerical modeling studies have been performed to study processes associated with specific storms along the Atlantic coasts (e.g., Virginia: Castagno et al., 2018; Zhu & Wiberg, 2022; New York: Hu et al., 2018), focused primarily on sediment transport trends.

In contrast, there have been several large-scale field investigations along the Louisiana coastal plain, looking at sedimentation related to Hurricanes Rita and Katrina (e.g., Baustian & Mendelssohn, 2015; McKee & Cherry, 2009; R. E. Turner et al., 2006) and Gustav and Ike (Tweel & Turner, 2012) as well as some smaller-scale investigations along a subset of the Gulf Coast, including Old Oyster Bayou and Bayou Chitigue, Louisiana (Cahoon et al., 1995) and Waccasassa Bay, Florida (Goodbred & Hine, 1995). There have also been attempts to relate individual frontal systems or seasonal stormy periods to event sedimentation (Cortese et al., 2024; Reed, 1989; R. S. Smith et al., 2024). In addition, several numerical modeling studies have been performed to analyze storm parameters for the US Gulf Coast (e.g., Georgiou, FitzGerald, & Hanegan, 2024; Liu et al., 2018).

Gulf Coast studies have demonstrated that hurricanes create sedimentary deposits covering expansive areas ranging in thickness from 0 to 30 cm (average ∼5 cm) (R. E. Turner et al., 2006; Tweel & Turner, 2012). Investigators have related the volumes of sediment moved and thickness of the resulting deposits to storm intensity, storm track, speed, duration, and wave energy (Georgiou, FitzGerald, & Hanegan, 2024; Liu et al., 2018) (see Table 2). Gulf Coast marshes and wetlands are fronted by shallow muddy open-water bays (10–20 km in width), and thus, during intense storms, ocean and local wind-generated waves induce high near-bed shear stresses and significant quantities of suspended sediment (Georgiou, FitzGerald, & Hanegan, 2024; Liu et al., 2018). Large storm surges accompanying these storms can extend far inland, carrying suspended sediment >50 km across marsh and wetlands (R. E. Turner et al., 2006; Tweel & Turner, 2012).

The physical setting of the Gulf is substantively different from that of the southeast Atlantic seaboard, where barrier-island chains front broad backbarrier marsh platforms incised by channels and tidal creeks with small attendant bays and tidal flats (M. O. Hayes, 1994). During storms, ocean waves are dampened as they propagate through tidal inlets, and at many locations, suspension of bottom sediment occurs by shear stresses created by local wind-generated waves combined with ambient tidal currents. As a result, Gulf Coast hurricanes, which are also typically larger in magnitude than those impacting the Georgia Bight, produce an average sediment thickness (5 cm) that is more than double the average Irma deposit (2.3 cm, Table 2). Further, these deposits differ in sediment texture because of differences in the source sediments. The large shallow bays situated seaward of Louisiana marshes evolved largely from inter-distributary bays, and thus contain primarily fine-grained sediment (Fisk & McFarlan, 1955; Frazier, 1967, 1974). Conversely, sand bodies floor much of the open-water area inside tidal inlets and extend far up tidal channels (M. O. Hayes, 1994; Howard & Frey, 1985). Considering these source

Table 2
Measurements of Hurricane-Deposit Thicknesses From Salt Marshes Within the US Gulf and Atlantic Coasts

Location	Hurricane, year	Wetland type	Sediment thickness [cm] (* Modeled)	Reference
East Coast				
Cedar Island, NC	Emily 1993	*Juncus*	0.3–0.4	Cahoon (2003)
Cedar Island, NC	Gordon 1994	*Juncus*	0.3–0.4	Cahoon et al. (1998)
Ochlockonee, Bald Pt, FL	Erin 1995	*Juncus*	0.5	Hendrickson (1997)
Cedar Island, NC	Dennis 1999	*Juncus*	0.8	Cahoon (2003)
Jamaica Bay Estuary, NY	Sandy 2012	*Spartina, Distichlis, Juncus*	1.5 *	Hu et al. (2018)
Barnegat Bay-Little Egg Harbor, NJ	Sandy 2012		0–1.4 *	Defne et al. (2019)
Amelia Island, FL	Irma 2017	*Spartina*	2.7	This study
Sapelo Island, GA	Irma 2017	*Spartina*	3.5	This study
Hilton Head, SC	Irma 2017	*Spartina*	2.16	This study
Cape Romain, SC	Irma 2017	*Spartina*	1	This study
Gulf Coast				
Old Oyster Bayou, LA	Andrew 1992	*Spartina*	2	Cahoon et al. (1995)
Bayou Chitigue, LA	Andrew 1992	*Spartina*	2.8	Cahoon et al. (1995)
Coastal Louisiana	Katrina and Rita 2005	*Spartina*	5.1	R. E. Turner et al. (2006)
Big Branch, LA	Katrina 2005	*Spartina*	0.1–4.5	McKee and Cherry (2009)
Pearl River, MS	Katrina 2005	*Spartina*	3.7–12.7	McKee and Cherry (2009)
Coastal Louisiana	Gustav 2008	*Spartina*	2	Tweel and Turner (2012)
Coastal Louisiana	Gustav and Ike 2008	*Spartina Germinans*	0.6–5.6	McKee et al. (2020)
Grand Bay Estuary, MS-AL	Nate 2017	*Juncu Spartina*	0.1–0.4	K. E. Smith et al. (2021)

Note. Marsh type is identified according to the dominant species, which, in general can be used as a measure of elevation to mean high water and rate of inundation as discussed in Mitsch and Gosselink (2015).

differences, our finding that the sediment comprising Irma deposits contains much greater sand percentages than those described along the muddy Gulf Coast is unsurprising.

In their study of storm deposits associated with Hurricanes Katrina (August. 2005), Rita (September 2005), and Gustav (September 2008), Tweel and Turner (2012) observed that storm deposits generally thinning and fined in a landward direction, which they related to dissipation in storm surge flow. In contrast, our results reveal no clear cross-shore trends across each of the backbarrier systems. We relate this to the differing physical conditions in these barrier-associated marshes, including the size of the open water source area, substrate variability, and spatially variable wave energy. The lack of any cross-shore trend compared to that recorded for Louisiana (Tweel & Turner, 2012) can be explained by the different physical conditions, including the size of the open water area, substrate variability, and spatially variable wave energy.

5.3. Role of Storm-Sedimentation on Long-Term Marsh Survival

While it is understood that storms are expected to increase in both frequency and intensity due to climate change (Knutson et al., 2015; Kossin et al., 2020), it is less well known how these changes will impact marsh vertical accretion and their resilience in the face of climate change and SLR. Modeling studies have found that stronger (e.g., Georgiou, FitzGerald, Sakib, et al., 2024; Pannozzo et al., 2021) and more frequent storms are expected to benefit marshes (Schuerch et al., 2013), and that even recurring moderate storms (Cortese et al., 2024) will enhance delivery of new sediment to the marsh (J. E. Smith et al., 2015). Still, studies of hurricane sedimentation along the Gulf Coast (e.g., McKee & Cherry, 2009; R. E. Turner et al., 2006; Tweel & Turner, 2012), this study of Irma deposits along the Georgia Bight, and a study of intense winter storms in New England (FitzGerald et al., 2020) all demonstrate that marshes can strongly benefit from sedimentation during extremely high energy events as a single large storm can deliver conspicuous volumes of mineral sediment (up to 10 cm in depth) to the marsh platform.

At the same marshes as in this study, Hein et al. (2024) reported multi-decadal accretion rates (using ^{210}Pb dating, see Table S4 in Supporting Information S1), ranging from 1.66 to >10 mm/yr (average = 5.37 mm/yr). These rates were retrieved from cores collected adjacent to our storm deposit samples, along the periphery of marsh platforms, but inboard of any existing levees. Comparison with other regional measurements of accretion demonstrated that these marsh edges accrete at far higher rates than adjoining marsh interiors (Hein et al., 2024). Comparison of these accretion rates with storm deposit thickness from the same locations reveals that an individual storm event can supply a sediment layer equivalent to about 3–4 years of pre-compaction accretion. A comparison of our event-related deposit thickness to the long-term accretion rates at the same sites also highlights how, even though this approximation does not account for further dewatering and compaction of the deposit or the addition of new biomass volume, it still indicates a considerable boost in elevation. Those stations demonstrating both fastest long-term accretion and greatest Irma deposit thickness are situated at highly exposed locations near tidal inlets or bays with substantial fetch. Thus, our findings are aligned with those from Hein et al. (2024) and build upon them, suggesting that vertical marsh resilience in these backbarrier settings stems in part from the delivery of sediment during high-energy events, a process aided by exposure to high wind and wave energy.

6. Conclusions

Analysis of 37 post-Hurricane Irma (2017) marsh cores obtained behind four barriers stretching from northern Florida to central South Carolina demonstrates that hurricanes can deliver significant mineral sediment during a single event, which can help marshes combat submergence. Irma deposits were found in 32 of 37 locations, decreasing in thickness and extent with distance from the storm's pathway, from a high of 8.0 cm at Sapelo Island to a low of 0 cm at some sites in Cape Romain and Hilton Head. This trend coincided with an overall decrease in wind velocities and wave energy from south to north, as indicated by modeling storm hydrodynamics. Unlike trends found during hurricane sedimentation studies in the Gulf Coast, our results lacked cross-shore trends in thickness or sand–mud content, suggesting that sediment transport onto the marsh surface is a function of site-specific tidal and wave-induced bottom shear stresses and substrate type. Several stations proximal to tidal inlets exhibited higher sand content, suggesting that ocean waves propagating into channels can enhance sediment entrainment and transport. Simultaneously, sites near tidal inlets or bays with greater wind and wave fetch show both the fastest accretion and thickest storm deposits, underscoring the role of high-energy sediment delivery in marsh resilience. Although the iterative multivariate regression analysis revealed only a weak relationship between thickness and wave energy, sand–mud ratio, and duration of storm inundation, we found a strong positive correlation between storm-deposit thickness and long-term accretion, indicating that high-energy events are a key driver of vertical marsh growth. Additional work is needed to evaluate hurricane-driven sedimentation across the interior marsh platform (e.g., Baustian & Mendelssohn, 2015; Tweel & Turner, 2012). Nonetheless, our findings have implications for how backbarrier systems with small internal open water bodies undergo hurricane sedimentation, implying that locally suspended material is important to marsh edge accretion.

Acknowledgments
The authors would like to acknowledge the contributions to laboratory work provided by Jennifer Saylor (nee Connell), Mahinaokalani Robbins (Virginia Institute of Marine Science), Ryen Guthrie (Boston University), and Tara Yocum and Michael Brown (University of New Orleans) for assistance with field sampling logistics. We extend our gratitude to Ovel Diaz Garcia for assisting in the analysis of modeling output for storm surge and wave energy. We thank the Georgia Coastal Ecosystem LTER and the University of Georgia Marine Institute at Sapelo Island for their support. GCE-LTER is supported by NSD award OCE-1832178. This work is UGAMI contribution number 1133. This work was funded by: National Science Foundation Geomorphology and Land Use Dynamics Program, award numbers: EAR-2022934, EAR-1800810 [RAPID], and EAR-1904470 [RAPID] in support of Duncan FitzGerald, Zoe Hughes and Alice Staro; award numbers: EAR-1800825 [RAPID], EAR-1904496 [RAPID], and EAR-2022987 in support of Christopher Hein; and award number: EAR-2022982 in support of Ioannis Georgiou. Partial funding was provided to Alice Staro by the Boston University Women's Council Scholarship. This work is a contribution to IGCP Project 725 “Forecasting Coastal Change.”

Conflict of Interest

The authors declare no conflicts of interest relevant to this study.

Availability Statement

Statistical analyses were performed using the Python libraries *Statsmodels* (Seabold & Perktold, 2010) and *Scikit-learn* (Pedregosa et al., 2011). Maps and spatial visualizations have been created in ArcGIS Pro 3.0.3 (Esri, 2022).

Data supporting this study are available from Staro et al. (2026).

References

Allen, J. (2000). Morphodynamics of Holocene salt marshes: A review sketch from the Atlantic and southern North Sea coasts of Europe. *Quaternary Science Reviews*, *19*(12), 1155–1231. https://doi.org/10.1016/s0277-3791(99)00034-7

Balaguru, K., Xu, W., Chang, C.-C., Leung, L. R., Judi, D. R., Hagos, S. M., et al. (2023). Increased U.S. coastal hurricane risk under climate change. *Science Advances*, *9*(14), eadf0259. https://doi.org/10.1126/sciadv.adf0259

Barbier, E. B., Hacker, S. D., Kennedy, C., Koch, E. W., Stier, A. C., & Silliman, B. R. (2011). The value of estuarine and coastal ecosystem services. *Ecological Monographs*, *81*(2), 169–193. https://doi.org/10.1890/10-1510.1

Baustian, J. J., & Mendelssohn, I. A. (2015). Hurricane-induced sedimentation improves marsh resilience and vegetation vigor under high rates of relative sea level rise. *Wetlands*, *35*(4), 795–802. https://doi.org/10.1007/s13157-015-0670-2

Baustian, J. J., & Mendelssohn, I. A. (2018). Sea level rise impacts to coastal marshes may be ameliorated by natural sedimentation events. *Wetlands*, *38*(4), 689–701. https://doi.org/10.1007/s13157-018-1012-y

Bendoni, M., Francalanci, S., Cappietti, L., & Solari, L. (2014). On salt marshes retreat: Experiments and modeling toppling failures induced by wind waves: Modeling salt marsh retreat. *Journal of Geophysical Research: Earth Surface*, *119*(3), 603–620. https://doi.org/10.1002/2013jf002967

Bendoni, M., Georgiou, I. Y., Roelvink, D., & Oumeraci, H. (2019). Numerical modelling of the erosion of marsh boundaries due to wave impact. *Coastal Engineering*, *152*, 103514. https://doi.org/10.1016/j.coastaleng.2019.103514

Bengtsson, L., Hodges, K. I., Esch, M., Keenlyside, N., Kornblueh, L., Luo, J.-J., & Yamagata, T. (2007). How may tropical cyclones change in a warmer climate? *Tellus A: Dynamic Meteorology and Oceanography*, *59*(4), 539–561. https://doi.org/10.1111/j.1600-0870.2007.00251.x

Bloemendaal, L. J. H., FitzGerald, D. M., Hughes, Z. J., Novak, A. B., & Phippen, P. (2021). What controls marsh edge erosion? *Geomorphology*, *386*, 107745. https://doi.org/10.1016/j.geomorph.2021.107745

Booij, N., Ris, R. C., & Holthuijsen, L. H. (1999). A third-generation wave model for coastal regions: 1. Model description and validation. *Journal of Geophysical Research*, *104*(C4), 7649–7666. https://doi.org/10.1029/98jc02622

Brandon, C. M., Woodruff, J. D., Donnelly, J. P., & Sullivan, R. M. (2014). How unique was hurricane sandy? Sedimentary reconstructions of extreme flooding from New York harbor. *Scientific Reports*, *4*(1), 7366. https://doi.org/10.1038/srep07366

Cahoon, D. R. (2003). Storms as agents of wetland elevation change: Their impact on surface and subsurface sediment processes. *Proceedings of the International Conference on Coastal Sediments*.

Cahoon, D. R. (2006). A review of major storm impacts on coastal wetland elevations. *Estuaries and Coasts*, *29*(6), 889–898. https://doi.org/10.1007/bf02798648

Cahoon, D. R., Day, J. W., Jr., Reed, D. J., & Young, R. S. (1998). Global climate change and sea level rise: Estimating the potential for submergence of coastal wetlands. In G. R. Guntenspergen & B. A. Vairin (Eds.), *Vulnerability of coastal wetlands in the southeastern United States: Climate change research results, 1992–1997 (biological science report USGS/BRD/BSR-1998-0002* (pp. 19–32). U.S. Geological Survey.

Cahoon, D. R., Olker, J. H., Yeates, A. G., Guntenspergen, G. R., Grace, J. B., Adamowicz, S. C., et al. (2019). *Hurricane sandy impacts on coastal wetland resilience*. U.S. Geological Survey.

Cahoon, D. R., Reed, D. J., Day, J. W., Jr., Steyer, G. D., Boumans, R. M., Lynch, J. C., et al. (1995). The influence of hurricane Andrew on sediment distribution in Louisiana coastal marshes. *Journal of Coastal Research*, 280–294.

Cangialosi, J. P., Latto, A. S., & Berg, R. (2018). *National hurricane center tropical cyclone report: Hurricane Irma* (pp. 1–111). National Hurricane Center.

Castagno, K. A., Donnelly, J. P., & Woodruff, J. D. (2021). Grain-size analysis of hurricane-induced event beds in a new England salt marsh, Massachusetts, USA. *Journal of Coastal Research*, *37*(2). https://doi.org/10.2112/jcoastres-d-19-00159.1

Castagno, K. A., Jiménez-Robles, A. M., Donnelly, J. P., Wiberg, P. L., Fenster, M. S., & Fagherazzi, S. (2018). Intense storms increase the stability of tidal bays. *Geophysical Research Letters*, *45*(11), 5491–5500. https://doi.org/10.1029/2018gl078208

Chaumillon, E., Bertin, X., Fortunato, A. B., Bajo, M., Schneider, J.-L., Dezileau, L., et al. (2017). Storm-induced marine flooding: Lessons from a multidisciplinary approach. *Earth-Science Reviews*, *165*, 151–184. https://doi.org/10.1016/j.earscirev.2016.12.005

Cherry, J. A., McKee, K. L., & Grace, J. B. (2009). Elevated CO2 enhances biological contributions to elevation change in coastal wetlands by offsetting stressors associated with sea-level rise. *Journal of Ecology*, *97*(1), 67–77. https://doi.org/10.1111/j.1365-2745.2008.01449.x

Chmura, G. L., Anisfeld, S. C., Cahoon, D. R., & Lynch, J. C. (2003). Global carbon sequestration in tidal, saline wetland soils. *Global Biogeochemical Cycles*, *17*(4). https://doi.org/10.1029/2002gb001917

Chowdhury, M. S. N., Walles, B., Sharifuzzaman, S., Shahadat Hossain, M., Ysebaert, T., & Smaal, A. C. (2019). Oyster breakwater reefs promote adjacent mudflat stability and salt marsh growth in a monsoon dominated subtropical coast. *Scientific Reports*, *9*(1), 8549. https://doi.org/10.1038/s41598-019-44925-6

Collins, E., Scott, D., & Gayes, P. (1999). Hurricane records on the South Carolina coast: Can they be detected in the sediment record? *Quaternary International*, *56*(1), 15–26. https://doi.org/10.1016/s1040-6182(98)00013-5

Contreras, M. T., Woods, B., Blakely, C., Wirasaet, D., Westerink, J., Cobell, Z., et al. (2023). A channel-to-basin scale ADCIRC based hydrodynamic unstructured mesh model for the US East and Gulf of Mexico coasts.

Cortese, L., Zhang, X., Simard, M., & Fagherazzi, S. (2024). Storm impacts on mineral mass accumulation rates of coastal marshes. *Journal of Geophysical Research: Earth Surface*, *129*(3), e2023JF007065. https://doi.org/10.1029/2023jf007065

Dallimore, A., Thomson, R. E., & Bertram, M. A. (2005). Modern to late Holocene deposition in an anoxic fjord on the west coast of Canada: Implications for regional oceanography, climate and paleoseismic history. *Marine Geology*, *219*(1), 47–69. https://doi.org/10.1016/j.margeo.2005.05.003

de Boer, G. B., de Weerd, C., Thoenes, D., & Goossens, H. W. (1987). Laser diffraction spectrometry: Fraunhofer diffraction versus Mie scattering. *Particle & Particle Systems Characterization*, *4*(1–4), 14–19. https://doi.org/10.1002/ppsc.19870040104

Defne, Z., Ganju, N. K., & Moriarty, J. M. (2019). Hydrodynamic and morphologic response of a back-barrier estuary to an extratropical storm. *Journal of Geophysical Research: Oceans*, *124*(11), 7700–7717. https://doi.org/10.1029/2019jc015238

de Groot, A. V., Veeneklaas, R. M., & Bakker, J. P. (2011). Sand in the salt marsh: Contribution of high-energy conditions to salt-marsh accretion. *Marine Geology*, *282*(3–4), 240–254. https://doi.org/10.1016/j.margeo.2011.03.002

Elsey-Quirk, T. (2016). Impact of Hurricane Sandy on salt marshes of New Jersey. *Estuarine, Coastal and Shelf Science*, *183*, 235–248. https://doi.org/10.1016/j.ecss.2016.09.006

Emanuel, K. A. (2013). Downscaling CMIP5 climate models shows increased tropical cyclone activity over the 21st century. *Proceedings of the National Academy of Sciences*, *110*(30), 12219–12224. https://doi.org/10.1073/pnas.1301293110

Enwright, N. M., Griffith, K. T., & Osland, M. J. (2016). Barriers to and opportunities for landward migration of coastal wetlands with sea-level rise. *Frontiers in Ecology and the Environment*, *14*(6), 307–316. https://doi.org/10.1002/fee.1282

Esri. (2022). ArcGIS Pro (version 3.0.3) [Software]. *Esri*. Retrieved from https://www.esri.com/arcgis-blog/products/arcgis-pro/

Fagherazzi, S., Mariotti, G., Wiberg, P. L., & McGlathery, K. J. (2013). Marsh collapse does not require sea level rise. *Oceanography*, *26*(3), 70–77. https://doi.org/10.5670/oceanog.2013.47

Feagin, R. A., Lozada-Bernard, S. M., Ravens, T. M., Möller, I., Yeager, K. M., & Baird, A. H. (2009). Does vegetation prevent wave erosion of salt marsh edges? *Proceedings of the National Academy of Sciences*, *106*(25), 10109–10113. https://doi.org/10.1073/pnas.0901297106

Fisk, H. N., & McFarlan, E., Jr. (1955). Late Quaternary deltaic deposits of the mississippi River: (local sedimentation and Basin tectonics). In A. Poldervaart (Ed.), *Crust of the Earth: A symposium* (Vol. 62, pp. 279–302). Geological Society of America. https://doi.org/10.1130/SPE62-p279

FitzGerald, D. M., Hughes, Z., Georgiou, I., Black, S., & Novak, A. (2020). Enhanced, climate-driven sedimentation on salt marshes. *Geophysical Research Letters*, *47*(10), e2019GL086737. https://doi.org/10.1029/2019gl086737

FitzGerald, D. M., Fenster, M. S., Argow, B. A., & Buynevich, I. V. (2008). Coastal impacts due to sea-level rise. *Annual Review of Earth and Planetary Sciences*, *36*(1), 601–647. https://doi.org/10.1146/annurev.earth.35.031306.140139

FitzGerald, D. M., Hein, C. J., Connell, J. E., Hughes, Z. J., Georgiou, I. Y., & Novak, A. B. (2021). Largest marsh in New England near a precipice. *Geomorphology*, *379*, 107625. https://doi.org/10.1016/j.geomorph.2021.107625

FitzGerald, D. M., & Hughes, Z. (2019). Marsh processes and their response to climate change and sea-level rise. *Annual Review of Earth and Planetary Sciences*, *47*(1), 481–517. https://doi.org/10.1146/annurev-earth-082517-010255

Folk, R. L. (1954). The distinction between grain size and mineral composition in sedimentary-rock nomenclature. *The Journal of Geology*, *62*(4), 344–359. https://doi.org/10.1086/626171

Frazier, D. E. (1967). Recent deltaic deposits of the Mississippi River: Their development and chronology.

Frazier, D. E. (1974). Depositional-episodes: Their relationship to the quaternary stratigraphic framework in the northwestern portion of the Gulf Basin.

Ganju, N. K., Defne, Z., Kirwan, M. L., Fagherazzi, S., D'Alpaos, A., & Carniello, L. (2017). Spatially integrative metrics reveal hidden vulnerability of microtidal salt marshes. *Nature Communications*, *8*(1), 14156. https://doi.org/10.1038/ncomms14156

Gardner, L. R., Michener, W. K., & Kjerfve, B. (1991). The geomorphic effects of Hurricane Hugo on an undeveloped coastal landscape at North Inlet, South Carolina. *Journal of Coastal Research*, *8*(2), 181–186.

Georgiou, I. Y., & Diaz Garcia, O. (2025). Time series model output from ADCIRC-SWAN simulation of Hurricane Irma (2017) along the Atlantic Seaboard used for correlating hurricane deposit thickness [Dataset]. *Zenodo*. https://doi.org/10.5281/ZENODO.16284832

Georgiou, I. Y., FitzGerald, D. M., & Hanegan, K. C. (2024). Storm and tidal interactions control sediment exchange in mixed-energy coastal systems. *PNAS Nexus*, *3*(2), pgae042. https://doi.org/10.1093/pnasnexus/pgae042

Georgiou, I. Y., FitzGerald, D. M., Sakib, M. M., Messina, F., Kulp, M. A., & Miner, M. D. (2024). Storm dynamics control sedimentation and shelf-bay-marsh sediment exchange along the Louisiana Coast. *Geophysical Research Letters*, *51*(22), e2024GL111344. https://doi.org/10.1029/2024GL111344

Goni, M. A., Alleau, Y., Corbett, R., Walsh, J. P., Mallinson, D., Allison, M. A., et al. (2007). The effects of hurricanes Katrina and Rita on the seabed of the Louisiana Shelf. *The Sedimentary Record*, *5*(1), 4–9. https://doi.org/10.2110/sedred.2007.1.4

Goodbred, S. L., Jr., & Hine, A. C. (1995). Coastal storm deposition: Salt-marsh response to a severe extratropical storm, March 1993, west-central Florida. *Geology*, *23*(8), 679–682. https://doi.org/10.1130/0091-7613(1995)023<0679:csdsmr>2.3.co;2

Gori, A., Lin, N., Xi, D., & Emanuel, K. (2022). Tropical cyclone climatology change greatly exacerbates US extreme rainfall–surge hazard. *Nature Climate Change*, *12*(2), 171–178. https://doi.org/10.1038/s41558-021-01272-7

Grigal, D. F., Brovold, S. L., Nord, W. S., & Ohmann, L. F. (1989). Bulk density of surface soils and peat in the North Central United States. *Canadian Journal of Soil Science*, *69*(4), 895–900. https://doi.org/10.4141/cjss89-092

Hayes, M. (1979). Barrier island morphology as a function of tidal and wave regime. In S. P. Leatherman (Ed.), *Barrier Islands* (Vol. 1, p. 27). Academic Press.

Hayes, M. O. (1994). The Georgia bight barrier system. In *Geology of Holocene barrier island systems* (pp. 233–304). Springer.

Hein, C. J., Connell, J. E., FitzGerald, D. M., Georgiou, I. Y., Hughes, Z. J., & King, K. (2024). Vertical accretion trends project doughnut-like fragmentation of saltmarshes. *Communications Earth & Environment*, *5*(1), 74. https://doi.org/10.1038/s43247-024-01219-8

Hein, C. J., & Kirwan, M. L. (2024). Marine transgression in modern times. *Annual Review of Marine Science*, *16*(1), 55–79. https://doi.org/10.1146/annurev-marine-022123-103802

Heiri, O., Lotter, A. F., & Lemcke, G. (2001). Loss on ignition as a method for estimating organic and carbonate content in sediments: Reproducibility and comparability of results. *Journal of Paleolimnology*, *25*(1), 101–110. https://doi.org/10.1023/a:1008119611481

Hendrickson, J. C. (1997). *Coastal wetland response to rising sea-level: Quantification of short-and long-term accretion and subsidence, northeastern Gulf of Mexico [PhD Thesis]*. Florida State University.

Hopkinson, C. S., Morris, J. T., Fagherazzi, S., Wollheim, W. M., & Raymond, P. A. (2018). Lateral marsh edge erosion as a source of sediments for vertical marsh accretion. *Journal of Geophysical Research: Biogeosciences*, *123*(8), 2444–2465. https://doi.org/10.1029/2017jg004358

Howard, J. D., & Frey, R. W. (1985). Physical and biogenic aspects of backbarrier sedimentary sequences, Georgia Coast, U.S.A. *Marine Geology*, *63*(1–4), 77–127. https://doi.org/10.1016/0025-3227(85)90080-5

Howes, N. C., FitzGerald, D. M., Hughes, Z. J., Georgiou, I. Y., Kulp, M. A., Miner, M. D., et al. (2010). Hurricane-induced failure of low salinity wetlands. *Proceedings of the National Academy of Sciences*, *107*(32), 14014–14019. https://doi.org/10.1073/pnas.0914582107

Hu, K., Chen, Q., Wang, H., Hartig, E. K., & Orton, P. M. (2018). Numerical modeling of salt marsh morphological change induced by Hurricane Sandy. *Coastal Engineering*, *132*, 63–81. https://doi.org/10.1016/j.coastaleng.2017.11.001

Jeffrey, D. W. (1970). A note on the use of ignition loss as a means for the approximate estimation of soil bulk density. *Journal of Ecology*, *58*(1), 297–299. https://doi.org/10.2307/2258183

Jevrejeva, S., Jackson, L., Grinsted, A., Lincke, D., & Marzeion, B. (2018). Flood damage costs under the sea level rise with warming of 1.5 C and 2 C. *Environmental Research Letters*, *13*(7), 074014. https://doi.org/10.1088/1748-9326/aacc76

King, K., Hein, C. J., FitzGerald, D. M., Hughes, Z. J., Georgiou, I. Y., & Connell, J. E. (2019). Saltmarsh event sedimentation: A comparative Study of hurricane IRMA deposits across the Southeast USA. *Geological Society of America Abstracts*, *51*, 326988.

Kirwan, M. L., & Guntenspergen, G. R. (2010). Influence of tidal range on the stability of coastal marshland. *Journal of Geophysical Research*, *115*(F2). https://doi.org/10.1029/2009jf001400

Kirwan, M. L., & Megonigal, J. P. (2013). Tidal wetland stability in the face of human impacts and sea-level rise. *Nature*, *504*(7478), 53–60. https://doi.org/10.1038/nature12856

Kirwan, M. L., Temmerman, S., Skeehan, E. E., Guntenspergen, G. R., & Fagherazzi, S. (2016). Overestimation of marsh vulnerability to sea level rise. *Nature Climate Change*, *6*(3), 253–260. https://doi.org/10.1038/nclimate2909

Kitsikoudis, V., Kibler, K. M., & Walters, L. J. (2020). In-situ measurements of turbulent flow over intertidal natural and degraded oyster reefs in an estuarine lagoon. *Ecological Engineering*, *143*, 105688. https://doi.org/10.1016/j.ecoleng.2019.105688

Knutson, T. R., Sirutis, J. J., Zhao, M., Tuleya, R. E., Bender, M., Vecchi, G. A., et al. (2015). Global projections of intense tropical cyclone activity for the late twenty-first century from dynamical downscaling of CMIP5/RCP4. 5 scenarios. *Journal of Climate*, *28*(18), 7203–7224. https://doi.org/10.1175/jcli-d-15-0129.1

Kossin, J. P. (2018). A global slowdown of tropical-cyclone translation speed. *Nature*, *558*(7708), 104–107. https://doi.org/10.1038/s41586-018-0158-3
Kossin, J. P., Knapp, K. R., Olander, T. L., & Velden, C. S. (2020). Global increase in major tropical cyclone exceedance probability over the past four decades. *Proceedings of the National Academy of Sciences*, *117*(22), 11975–11980. https://doi.org/10.1073/pnas.1920849117
Kulp, S. A., & Strauss, B. H. (2019). New elevation data triple estimates of global vulnerability to sea-level rise and coastal flooding. *Nature Communications*, *10*(1), 1–12. https://doi.org/10.1038/s41467-019-12808-z
Leonardi, N., & Fagherazzi, S. (2015). Effect of local variability in erosional resistance on large-scale morphodynamic response of salt marshes to wind waves and extreme events. *Geophysical Research Letters*, *42*(14), 5872–5879. https://doi.org/10.1002/2015gl064730
Liu, K., Chen, Q., Hu, K., Xu, K., & Twilley, R. R. (2018). Modeling hurricane-induced wetland-bay and bay-shelf sediment fluxes. *Coastal Engineering*, *135*, 77–90. https://doi.org/10.1016/j.coastaleng.2017.12.014
Luettich Jr, R. A., Westerink, J. J., & Scheffner, N. W. (1992). ADCIRC: An advanced three-dimensional circulation model for shelves, coasts, and estuaries. Report 1. Theory and methodology of ADCIRC-2DDI and ADCIRC-3DL.
Mann, M. E., & Emanuel, K. A. (2006). Atlantic hurricane trends linked to climate change. *EOS Transactions of the American Geophysical Union*, *87*(24), 233–241. https://doi.org/10.1029/2006eo240001
Marani, M., D'Alpaos, A., Lanzoni, S., & Santalucia, M. (2011). Understanding and predicting wave erosion of marsh edges: Marsh edge erosion. *Geophysical Research Letters*, *38*(21). https://doi.org/10.1029/2011gl048995
McKee, K. L., & Cherry, J. A. (2009). Hurricane Katrina sediment slowed elevation loss in subsiding brackish marshes of the Mississippi River delta. *Wetlands*, *29*(1), 2–15. https://doi.org/10.1672/08-32.1
McKee, K. L., Mendelssohn, I. A., & Hester, M. W. (2020). Hurricane sedimentation in a subtropical salt marsh-mangrove community is unaffected by vegetation type. *Estuarine, Coastal and Shelf Science*, *239*, 106733. https://doi.org/10.1016/j.ecss.2020.106733
Mitsch, W. J., & Gosselink, J. G. (2015). *Wetlands*. John Wiley & Sons.
Möller, I., Kudella, M., Rupprecht, F., Spencer, T., Paul, M., Van Wesenbeeck, B. K., et al. (2014). Wave attenuation over coastal salt marshes under storm surge conditions. *Nature Geoscience*, *7*(10), 727–731. https://doi.org/10.1038/NGEO2251
Morris, J. T., Barber, D. C., Callaway, J. C., Chambers, R., Hagen, S. C., Hopkinson, C. S., et al. (2016). Contributions of organic and inorganic matter to sediment volume and accretion in tidal wetlands at steady state. *Earth's Future*, *4*(4), 110–121. https://doi.org/10.1002/2015ef000334
Morris, J. T., Lynch, J., Renken, K. A., Stevens, S., Tyrrell, M., & Plaisted, H. (2020). Tidal and hurricane impacts on saltmarshes in the northeastern coastal and barrier network: Theory and empirical results. *Estuaries and Coasts*, *43*(7), 1658–1671. https://doi.org/10.1007/s12237-020-00790-5
Morris, J. T., Sundareshwar, P., Nietch, C. T., Kjerfve, B., & Cahoon, D. R. (2002). Responses of coastal wetlands to rising sea level. *Ecology*, *83*(10), 2869–2877. https://doi.org/10.1890/0012-9658(2002)083[2869:rocwtr]2.0.co;2
Morris, R. L., La Peyre, M. K., Webb, B. M., Marshall, D. A., Bilkovic, D. M., Cebrian, J., et al. (2021). Large-scale variation in wave attenuation of oyster reef living shorelines and the influence of inundation duration. *Ecological Applications*, *31*(6), e02382. https://doi.org/10.1002/eap.2382
Morton, R. A., & Barras, J. A. (2011). Hurricane impacts on coastal wetlands: A half-century record of storm-generated features from southern Louisiana. *Journal of Coastal Research*, *27*(6A), 27–43. https://doi.org/10.2112/jcoastres-d-10-00185.1
Moskalski, S. M., & Sommerfield, C. K. (2012). Suspended sediment deposition and trapping efficiency in a Delaware salt marsh. *Geomorphology*, *139–140*, 195–204. https://doi.org/10.1016/j.geomorph.2011.10.018
Mudroch, A., & Bourbonniere, R. A. (1994). Sediment preservation. *Handbook of Techniques for Aquatic Sediments Sampling*, *131*.
Muller, R. A., & Stone, G. W. (2001). A climatology of tropical storm and hurricane strikes to enhance vulnerability prediction for the southeast US coast. *Journal of Coastal Research*, 949–956.
Munsell, A. H. (2000). *Munsell soil color charts*. Gretagmacbeth.
National Hurricane Center. (2018). *2017 Atlantic hurricane season: Tropical cyclone reports*. National Oceanic and Atmospheric Administration. Retrieved from https://www.nhc.noaa.gov/data/tcr/index.php?season=2017&basin=atl
Nummedal, D. (1978). Tidal inlet variability-Cape hatteras to Cape Canaveral. In *Coastal sediments '77, 5th symposium of the waterway, port, coastal and Ocean division*. ASCE. Retrieved from https://cir.nii.ac.jp/crid/1573387450361307648
Nyman, J., DeLaune, R., Roberts, H., & Patrick, W. (1993). Relationship between vegetation and soil formation in a rapidly submerging coastal marsh. *Marine Ecology Progress Series*, *96*, 269–279. https://doi.org/10.3354/meps096269
Nyman, J. A., Crozier, C. R., & DeLaune, R. D. (1995). Roles and patterns of hurricane sedimentation in an estuarine marsh landscape. *Estuarine, Coastal and Shelf Science*, *40*(6), 665–679. https://doi.org/10.1006/ecss.1995.0045
Ouyang, X., & Lee, S. Y. (2020). Improved estimates on global carbon stock and carbon pools in tidal wetlands. *Nature Communications*, *11*(1), 317. https://doi.org/10.1038/s41467-019-14120-2
Pannozzo, N., Leonardi, N., Carnacina, I., & Smedley, R. (2021). Salt marsh resilience to sea-level rise and increased storm intensity. *Geomorphology*, *389*, 107825. https://doi.org/10.1016/j.geomorph.2021.107825
Pedregosa, F., Varoquaux, G., Gramfort, A., Michel, V., Thirion, B., Grisel, O., et al. (2011). Scikit-learn: Machine learning in python [Software]. *Journal of Machine Learning Research*, *12*, 2825–2830. http://scikit-learn.org/
Plater, A. J., Kirby, J. R., Boyle, J. F., Shaw, T., & Mills, H. (2015). Loss on ignition and organic content. *Handbook of Sea-Level Research*, 312–330.
Reed, D. J. (1989). Patterns of sediment deposition in subsiding coastal salt marshes, Terrebonne Bay, Louisiana: The role of winter storms. *Estuaries*, *12*(4), 222–227. https://doi.org/10.2307/1351901
Reynolds, T. (2024). Grain size from source to sink–modern and ancient fining rates. *Earth-Science Reviews*, *250*, 104699. https://doi.org/10.1016/j.earscirev.2024.104699
Ridge, J. T., Rodriguez, A. B., Joel Fodrie, F., Lindquist, N. L., Brodeur, M. C., Coleman, S. E., et al. (2015). Maximizing oyster-reef growth supports green infrastructure with accelerating sea-level rise. *Scientific Reports*, *5*(1), 14785. https://doi.org/10.1038/srep14785
Roman, C. T., Peck, J. A., Allen, J. R., King, J. W., & Appleby, P. G. (1997). Accretion of a New England (USA) salt marsh in response to inlet migration, storms, and sea-level rise. *Estuarine, Coastal and Shelf Science*, *45*(6), 717–727. https://doi.org/10.1006/ecss.1997.0236
Schuerch, M., Spencer, T., Temmerman, S., Kirwan, M. L., Wolff, C., Lincke, D., et al. (2018). Future response of global coastal wetlands to sea-level rise. *Nature*, *561*(7722), 231–234. https://doi.org/10.1038/s41586-018-0476-5
Schuerch, M., Vafeidis, A., Slawig, T., & Temmerman, S. (2013). Modeling the influence of changing storm patterns on the ability of a salt marsh to keep pace with sea level rise. *Journal of Geophysical Research: Earth Surface*, *118*(1), 84–96. https://doi.org/10.1029/2012jf002471
Schwimmer, R. A., & Pizzuto, J. E. (2000). A model for the evolution of marsh shorelines. *Journal of Sedimentary Research*, *70*(5), 1026–1035. https://doi.org/10.1306/030400701026

Scott, D., Collins, E., Gayes, P., & Wright, E. (2003). Records of prehistoric hurricanes on the South Carolina coast based on micropaleontological and sedimentological evidence, with comparison to other Atlantic Coast records. *Geological Society of America Bulletin*, *115*(9), 1027–1039. https://doi.org/10.1130/b25011.1

Seabold, S., & Perktold, J. (2010). Statsmodels: Econometric and statistical modeling with python [Software]. *9th Python in Science Conference*. https://proceedings.scipy.org/articles/Majora-92bf1922-011

Smith, J. E., Bentley, S. J., Snedden, G. A., & White, C. (2015). What role do hurricanes play in sediment delivery to subsiding river deltas? *Scientific Reports*, *5*(1), 17582. https://doi.org/10.1038/srep17582

Smith, K. E., Terrano, J. F., Khan, N. S., Smith, C. G., & Pitchford, J. L. (2021). Lateral shoreline erosion and shore-proximal sediment deposition on a coastal marsh from seasonal, storm and decadal measurements. *Geomorphology*, *389*, 107829. https://doi.org/10.1016/j.geomorph.2021.107829

Smith, R. S., Pennings, S. C., Alber, M., Craft, C., & Byers, J. E. (2024). The resistance of Georgia coastal marshes to hurricanes. *Ecosphere*, *15*(4), e4821. https://doi.org/10.1002/ecs2.4821

Sousa, A. I., Lillebø, A. I., Pardal, M. A., & Caçador, I. (2010). Productivity and nutrient cycling in salt marshes: Contribution to ecosystem health. *Estuarine, Coastal and Shelf Science*, *87*(4), 640–646. https://doi.org/10.1016/j.ecss.2010.03.007

Staro, A., FitzGerald, D., Georgiou, I., Hein, C., & Hughes, Z. (2026). Hurricanes along the Southeast Atlantic Coast build marsh resiliency through mineral sedimentation (Version v2) [Dataset]. *Zenodo*. https://doi.org/10.5281/zenodo.18378484

Stumpf, R. P. (1983). The process of sedimentation on the surface of a salt marsh. *Estuarine, Coastal and Shelf Science*, *17*(5), 495–508. https://doi.org/10.1016/0272-7714(83)90002-1

Styles, R. (2015). Flow and turbulence over an oyster reef. *Journal of Coastal Research*, *31*(4), 978–985. https://doi.org/10.2112/jcoastres-d-14-00115.1

Temmerman, S., Meire, P., Bouma, T. J., Herman, P. M., Ysebaert, T., & De Vriend, H. J. (2013). Ecosystem-based coastal defence in the face of global change. *Nature*, *504*(7478), 79–83. https://doi.org/10.1038/nature12859

Ting, M., Kossin, J. P., Camargo, S. J., & Li, C. (2019). Past and future hurricane intensity change along the US East Coast. *Scientific Reports*, *9*(1), 7795. https://doi.org/10.1038/s41598-019-44252-w

Torio, D. D., & Chmura, G. L. (2013). Assessing Coastal squeeze of tidal wetlands. *Journal of Coastal Research*, *290*, 1049–1061. https://doi.org/10.2112/jcoastres-d-12-00162.1

Tuit, C., & Wait, A. (2020). A review of marine sediment sampling methods. *Environmental Forensics*, *21*(3–4), 291–309. https://doi.org/10.1080/15275922.2020.1771630

Turner, R., Swenson, E., Milan, C., Weinstein, M., & Kreeger, D. (2002). Concepts and controversies in tidal marsh ecology.

Turner, R. E., Baustian, J. J., Swenson, E. M., & Spicer, J. S. (2006). Wetland sedimentation from hurricanes Katrina and Rita. *Science*, *314*(5798), 449–452. https://doi.org/10.1126/science.1129116

Tweel, A. W., & Turner, R. E. (2012). Landscape-Scale analysis of wetland sediment deposition from four tropical cyclone events. *PLoS One*, *7*(11), e50528. https://doi.org/10.1371/journal.pone.0050528

Van Rijn, L. C. (1984a). Sediment transport, part I: Bed load transport. *Journal of Hydraulic Engineering*, *110*(10), 1431–1456. https://doi.org/10.1061/(asce)0733-9429(1984)110:10(1431)

Van Rijn, L. C. (1984b). Sediment transport, part II: Suspended load transport. *Journal of Hydraulic Engineering*, *110*(11), 1613–1641. https://doi.org/10.1061/(asce)0733-9429(1984)110:11(1613)

Wentworth, C. K. (1922). A scale of grade and class terms for clastic sediments. *The Journal of Geology*, *30*(5), 377–392. https://doi.org/10.1086/622910

Westerink, J. J., Luettich Jr, R., Blain, C., & Scheffner, N. W. (1994). Adcirc: An advanced three-dimensional circulation model for shelves, coasts, and estuaries. Report 2. User's manual for adcirc-2ddi.

Weston, N. B. (2014). Declining sediments and rising Seas: An unfortunate convergence for tidal wetlands. *Estuaries and Coasts*, *37*(1), 1–23. https://doi.org/10.1007/s12237-013-9654-8

Whitman, E. R., & Reidenbach, M. A. (2012). Benthic flow environments affect recruitment of Crassostrea virginica larvae to an intertidal oyster reef. *Marine Ecology Progress Series*, *463*, 177–191. https://doi.org/10.3354/meps09882

Wiberg, P. L., Fagherazzi, S., & Kirwan, M. L. (2020). Improving predictions of Salt Marsh evolution through better integration of data and models. *Annual Review of Marine Science*, *12*(1), 389–413. https://doi.org/10.1146/annurev-marine-010419-010610

Woollings, T., Hoskins, B., Blackburn, M., Hassell, D., & Hodges, K. (2010). Storm track sensitivity to sea surface temperature resolution in a regional atmosphere model. *Climate Dynamics*, *35*(2–3), 341–353. https://doi.org/10.1007/s00382-009-0554-3

Wright, L., Gammisch, R., & Byrne, R. (1990). Hydraulic roughness and mobility of three oyster-bed artificial substrate materials. *Journal of Coastal Research*, 867–878.

Yeates, A. G., Grace, J. B., Olker, J. H., Guntenspergen, G. R., Cahoon, D. R., Adamowicz, S., et al. (2020). Hurricane sandy effects on coastal marsh elevation change. *Estuaries and Coasts*, *43*(7), 1640–1657. https://doi.org/10.1007/s12237-020-00758-5

Zhu, Q., & Wiberg, P. L. (2022). The importance of storm surge for sediment delivery to microtidal marshes. *Journal of Geophysical Research: Earth Surface*, *127*(9), e2022JF006612. https://doi.org/10.1029/2022jf006612

References From the Supporting Information

NDBC. (n.d.). Wind and wave data collected from National Data Buoy Center [Dataset]. Retrieved from https://www.ndbc.noaa.gov/

Planet Labs PBC. (2021). Planet application program interface: In space for life on Earth. San Francisco, CA. Retrieved from https://api.planet.com